On the hydrodynamic analysis of macromolecular conformation

Stephen E. Harding [*]

University of Nottingham, School of Agriculture, Sutton Bonington LE12 5RD, UK

Abstract

Hydrodynamics provides a powerful complementary role to the traditional "high resolution" techniques for the investigation of macromolecular conformation, especially in dilute solution, conditions which are generally inaccessible to other structural techniques. This paper describes the state of art of hydrodynamic representations for macromolecular conformation, in terms of (1) simple but straightforward ellipsoid of revolution modelling; (2) general triaxial ellipsoid modelling; (3) hydrodynamic bead modelling; (4) the ability, especially for polydisperse macromolecular systems, to distinguish between various conformation types; (5) analysis of macromolecular flexibility.

Keywords: Triaxial ellipsoid; Bead models; Polydispersity; Flexibility; Worm-like coil

1. Introduction

Hydrodynamic methods are now regaining a certain degree of fashionability amongst biomolecular scientists. Although forever they will carry the label of "low-resolution" status compared with X-ray crystallography, high-resolution nuclear magnetic resonance and molecular modelling there are many classes of macromolecule and macromolecular system where, low resolution or not, hydrodynamics plays the leading role. And indeed, these methods can provide an important supporting cast to the so-called "high" resolution techniques: in the case of nuclear magnetic resonance for example, because of the high concentrations on a mass/volume basis required to give satisfactory spectra, simple sedimentation velocity or equilibrium runs in the analytical ultracentrifuge can provide vital checks against any self-association behaviour which can give rise to

misinterpretation of the chemical shift or related spectra. Hydrodynamic methods are generally rapid and non-destructive: these particular features have not escaped the notice of for example molecular biologists who often have only very small amounts of precious material available. They can provide early "low resolution" information on a macromolecular structure prior to detailed crystallographic or high-resolution nuclear magnetic resonance analysis. Or, conversely, they can provide the finishing touches refining a crystallographic model to account for *dilute* solution behaviour, especially in terms of *inter*-molecular interaction phenomena [1]. The delicate *intra*-molecular relationships between subunits of a multi-enzyme complex can also be explored. In now almost classical work, H.K. Schachman and coworkers [2] showed, using a combination of high-precision analytical ultracentrifuge measurements with the tools of molecular biology (production of point mutants) how such interactions in aspartate transcarbamoylase produce powerful allostery.

[*] Corresponding author.

There have been many classic reviews on the application of hydrodynamic probes. Despite its age, C. Tanford's book of 1961 [3] is still regarded by many as the authority on the subject, although the subject has advanced considerably since this time, particularly in terms of hydrodynamic modelling (tri-axial ellipsoids, bead models, flexible particle analysis etc.). So, the purpose of this article is to attempt to describe the 1994 state of the art of hydrodynamic methodology for the investigation of macromolecular conformation in dilute solution. This article will be light on detailed mathematical expressions, since no new theory is presented, but some of the principal functions and relations will be given, and some key follow-up references given. This article will also be light on details concerning the experimental techniques but again the appropriate references will be given.

2. Hydrodynamic probes

The principal hydrodynamic probes for macromolecular conformation in solution are:
– intrinsic viscosity,
– sedimentation velocity,
– fluorescence depolarisation (both anisotropy decay and steady state),
– electric birefringence or dichroism decay,
– dynamic light scattering.

Even a simple technique like *viscometry* can give remarkably detailed information (in terms of general ellipsoid, rigid bead or flexibility modelling) and is still used by many groups – especially those working on polysaccharides and glycoconjugates. Most modern capillary viscometers involve automatic pumping and timing. The intrinsic viscosity $[\eta]$, from which shape information can be inferred is now most conveniently obtained from the common intercept of a dual extrapolation (Fig. 1a) to zero concentration, c, of the reduced viscosity, η_{red}, (Huggins plot) and the inherent viscosity, $\ln \eta_{rel}/c$ (Kraemer plot), where η_{rel} is the relative viscosity. For highly asymmetric macromolecules where molecular alignment even under the very small shear stresses in a capillary viscometer is a possibility (leading to an underestimate of $[\eta]$) a variety of automatic or semi-automatic cone-and-plate type viscometers, which permit
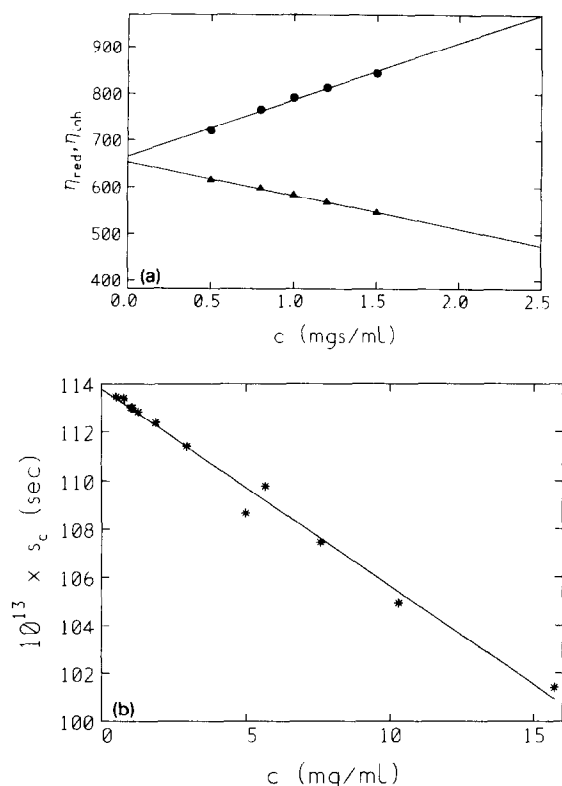

Fig. 1. Extraction of intrinsic viscosities and sedimentation coefficients. (a) Reduced viscosity, η_{red} (ml/g) versus concentration (●) and inherent viscosity, $\ln \eta_{rel} / c$ (ml/g) versus concentration (▲) for irradiated (10 kGy) guar in a phosphate–chloride buffer (pH = 6.8, I = 0.10) The "common" intercept gives $[\eta]$, the slopes are $K_H[\eta]^2$ and $K_K[\eta]^2$. K_H is the Huggins constant and K_K the Kraemer constant, respectively. From [4]. (b) Sedimentation coefficient, $s_{20,w}$ versus concentration plot for turnip yellow mosaic virus. The intercept gives $s_{20,w}^0$, the slope $s_{20,w}^0.k_s$, where k_s is the sedimentation concentration regression coefficient. Both $s_{20,w}^0$ and k_s give conformation information. From [5].

an extrapolation to zero shear rate, are now available [6].

Another relatively simple technique – *sedimentation velocity* analysis – can give valuable conformation information from plots of the sedimentation coefficient, $s_{20,w}$, against concentration (Fig. 1b). Modern instruments are now equipped with full online or off-line data capture and analysis facilities for both absorption and Rayleigh interference optics [7].

Dynamic light scattering instruments – for the rapid measurement of translational diffusion coefficients are now commonplace and the theory is well developed [8]. Although most of the recent attention
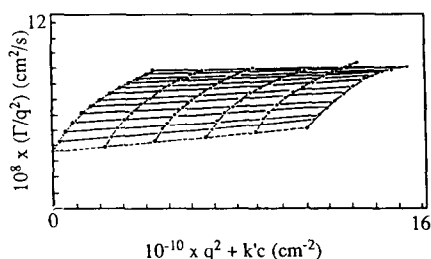
Fig. 2. Dynamic Zimm Plot. For a *Rhizobium trifolii* exopolysaccharide in 0.1M NaCl. $\Gamma = Dq^2$, with D being the translational diffusion coefficient and q the Bragg wave vector. k' is an arbitrary scaling constant. The slope of the zero angle line gives the concentration dependence diffusion parameter k_D ref. [5] explains the significance of this parameter). The slope of the zero concentration line can give information concerning flexibility of the macromolecule [11]. The common intercept gives the "infinite" dilution value, D^0, which when corrected to standard conditions (water as solvent at 20° C) gives $D^0_{20,w}$. From [11].

has been directed towards size-distribution analyses [9,10], one important development in terms of conformation analysis has been the establishment of a systematic way of correcting apparent translational diffusion (or the equivalent autocorrelation) data for concentration and angular dependence effects, using a biaxial extrapolation in a "dynamic" Zimm plot [11]. By analogy with the conventional Zimm plot from classical "static" or "integrated" light scattering [12] the common intercept (Fig. 2) gives the true translational diffusion coefficient without ambiguities. Much recent attention has been addressed to the extraction and use of the translational diffusion coefficient (especially in relation to the conformation of nucleic acids) and two recent edited volumes highlight this [8,13]. Some aspects of this will be considered later in this article. In terms of size distribution analysis of polydisperse systems (such as polysaccharides, glycoproteins, proteoglycans and nucleic acids), considerable progress has been made, and for example Johnsen and Brown [9] and Stepanek [10] have critically examined the various procedures available (based on for example Laplace transforms, cumulants analyses, lambda depression etc.), although because all these procedures ultimately involve the resolution of multi-exponential decay phenomena, and the difficulties therein, methods involving a physical (as opposed to a computational) separation are arguably superior. An example of this is

the coupling of gel permeation chromatography online to a multi-angle "static" (i.e. total intensity) light scattering photometer [14].

Rotational diffusion coefficients or relaxation times (which also have to be extrapolated to zero concentration [15]), are usually more sensitive functions of conformation compared with their corresponding translational counterparts, but this extra sensitivity comes unfortunately at a price – in terms of the greater difficulty in both making the measurements and in extracting the parameters. For measuring rotational diffusion coefficients (or equivalently rotational relaxation times) *electric birefringence* (or electric dichroism, especially if nucleic acids are being examined) decay [16] and *fluorescence depolarisation anisotropy decay* [17] remain as the principal probes, with arguably electric birefringence decay being the method of choice since for a given monodisperse solution of asymmetric scatterers there are just two exponentials to resolve [18] as opposed to five from fluorescence anisotropy decay [19]. Both involve the problem of deconvolution of source functions [16,20]. A further serious restriction of electric birefringence has been the restriction to solutions of low ionic strengths, because of heating effects caused by the strong electric fields used. The most significant recent advance in terms of electric birefringence/dichroism instrumentation has been the design of an instrument with adequate shielding against such effects by Pörschke [21] to permit the use of solvents at physiological ionic strengths, and this has for example been successfully applied to DNA restriction fragments. Finally, despite the drawbacks of the anisotropy decay technique, *steady state fluorescence depolarisation* methods can also be used as a conformation probe by the harmonic mean rotational relaxation time τ_h, and one of the best demonstrations of segmental flexibility in a molecule has been shown by Mihalyi and Johnson [22] using this technique.

The molar mass (or "molecular weight") M (g/mol) remains an important parameter in many of the equations involving hydrodynamic conformation parameters, but for monodisperse single subunit systems M can be obtained simply from sequence analysis or for molecular weights up to 10^5, and without the restrictions of monodispersity, from mass spectrometry [23]. For molecules containing more

Table 1
Hydrodynamic handles on conformation

Hydrodynamic model	Follow-up reference [a]
Ellipsoids of revolution	[27,28]
General triaxial ellipsoid	[29,28]
Bead models	[30,31]
General structures (Mark–Houwink–Kuhn–Sakurada coefficients, Wales–van Holde ratio, Haug triangle)	[32,33]
Flexibility analysis	[34,30]

[a] Source references can be found therein.

than one subunit, or of $M > 10^5$, sedimentation equilibrium analysis retains its usefulness [24]. The partial specific volume $\bar{v}$ also remains an important requisite parameter, and advances have also made here in its prediction from composition information [25], although density meters of the type described by Kratky et al. [26] are now more or less standard instruments for this purpose. An even more important parameter for hydrodynamic conformation analysis – the hydrated specific volume v_s (or equivalently the "hydration", w or δ) – still unfortunately remains elusive to pin down, and elaborate procedures for avoiding having to estimate it still have to be employed as will be discussed below.

3. The five hydrodynamic approaches to conformation analysis

Their are five modelling strategies for handling macromolecular conformation in solution (Table 1) ranging from simple ellipsoids of revolution modelling (which can be performed relatively quickly) at one extreme right through to quite sophisticated bead model representations (requiring usually several independent measurements to minimise non-uniqueness problems) and worm-like coil representations of particle flexibility at the other extreme. Each of the modelling strategies – the ellipsoid of revolution approach, the general triaxial ellipsoid approach, the bead model approach, "general structure" analysis and flexibility analysis – will now be considered in turn.

4. Ellipsoids of revolution

For a comprehensive description of this type of modelling the reader can consult Ref. [27] and the

original source references cited therein. The simplest model for particle conformation in solution is the rigid sphere and the earliest calculations were based on spherical particles in terms of their frictional properties (sedimentation or diffusion) *through* a solution [35] and on their effect on the bulk viscous properties *of* a solution [36,37]. In 1936 Perrin [38] extended Stokes' analyses to the case of general ellipsoids (of semi-axes $a \geq b \geq c$). Unfortunately, because of the complexity of the elliptic integrals involved macromolecules could only be modelled in terms of prolate or oblate "ellipsoids of revolution" with the restriction of two axes having to be equal. (The three semi-axes of a prolate ellipsoid (two equal minor axes) are a,b,b and for an oblate ellipsoid (two equal major axes) are a,a,b with the axial ratio $(a/b) \geq 1$ in both cases [1]). Nonetheless this meant that advantage could be taken of the advent of the analytical ultracentrifuge in the 1920's [39,40] which allowed the measurement of particle frictional ratios (f/f_0) (f is the frictional coefficient and f_0 is the corresponding coefficient of a spherical particle of the same mass and dry volume) from the sedimentation coefficient $s_{20,w}^0$ or the translational diffusion coefficient $D_{20,w}^0$.

$$(f/f_0) = \left(M(1 - \bar{v}\rho_0)/N_A \cdot 6\pi\eta_0 s_{20,w}^0 \right)$$
$$\times \left(4\pi N_A/3\bar{v}M\right)^{1/3} \tag{1}$$

or in terms of translational diffusion

$$(f/f_0) = \frac{k_B T}{6\pi\eta_0} \left(\frac{4\pi N_A}{3\bar{v}M} \right)^{1/3} \cdot \frac{1}{D_{20,w}^0} \tag{2}$$

----

[1] This is the Tanford [3] convention which is generally followed now. In some texts, the convention is used where an oblate ellipsoid has semi-axes b,b,a with $b \geq a$ (see Ref. [28]).

where N_A is Avogadro's number, M is the molar mass, $\bar{v}$ the partial specific volume, k_B is Boltzmann's constant and R the gas constant, T the absolute temperature and ρ_0 and η_0 are respectively the density and viscosity of water at 20.0° C. The subscripts 20,w mean after correction to standard conditions (water as solvent at 20° C) and the superscript "0" means after extrapolation to infinite dilution. In order to get shape information from (1) or (2) first of all a function P is defined (named in recognition of F. Perrin)

$$P = (f/f_0) \cdot (\bar{v}/v_s)^{1/3} \tag{3}$$

where v_s, the "hydrated" or "swollen" specific volume (ml/g) is the volume occupied by the macromolecule and associated solvent per unit mass of anhydrous macromolecule, and then the axial ratio of the ellipsoid, a/b (≥ 1) can be obtained from tables or graphs generated by the equations

$$P = \frac{\left(1 - b^2/a^2\right)^{1/2}}{(b/a)^{2/3} \ln \dfrac{1 + \left(1 - b^2/a^2\right)^{1/2}}{b/a}} \tag{4a}$$

(prolate ellipsoid), or for an oblate ellipsoid from

$$P = \frac{\left(a^2/b^2 - 1\right)^{1/2}}{(a/b)^{2/3} \tan^{-1}\left(a^2/b^2 - 1\right)^{1/2}} \tag{4b}$$

and so P as a function of a/b could be given (Fig. 3a). From the tabulated data worked out by Perrin and others, Laue et al. [41] have given the following polynomial approximation (accurate to ± 0.01 in the range $1 < a/b < 200$) for the inversion of Eq. (4):

$$(a/b) = 1 + 2.346 X^{1/2} + 8.297 X + 8.4 X^2$$
$$- 0.4589 X^3 + 0.0314 X^4 \tag{5a}$$

(prolate case) and

$$(a/b) = 1 + 2.975 X^{1/2} + 8.48 X + 13.295 X^2$$
$$- 3.219 X^3 + 0.0996 X^4 \tag{5b}$$

for the oblate case, where in both cases $X = P - 1$. Perrin [42] had also earlier given formulae for rotational diffusion coefficients and some of these "rotational" parameters, along with all the other important ellipsoid of revolution shape parameters worked out for ellipsoids of revolution are given in Table 2.

Table 2

Hydrodynamic shape parameters for ellipsoids of revolution (semi-axes a,b,b (prolate) and a,a,b (oblate) and $a \geq b$)

Shape parameter	Related experimental parameter	Reference
Bulk solution properties:		
Viscosity increment (ν)	Intrinsic viscosity [η]	[43,45,48]
Reduced molecular covolume (u_{red})	Thermodynamic 2nd virial coefficient, B or A_2 (from light scattering, sedimentation equilibrium etc.)	[49,50]
Translational frictional property:		
Perrin function (P)	Frictional ratio f/f_0 (and hence the sedimentation coefficient ($s_{20,w}^0$) and the translational diffusion coefficient ($D_{20,w}^0$))	[39,48]
Rotational frictional property [a]:		
"Reduced" birefringence (or dichroism) decay constant (θ^{red})	[b] Electric birefringence (or dichroism) decay constant (θ)	[51]
Harmonic mean rotational relaxation time ratio τ_h/τ_0	Harmonic mean rotational relaxation times (from steady state fluorescence depolarisation studies) (τ_h)	[52]
Fluorescence anisotropy depolarisation rotational relaxation time ratios (τ_i/τ_0; $i = 1$–3)	[c] Fluorescence anisotropy depolarisation relaxation times (τ_i)	[17]

The subscript "o" in f_0 means the corresponding coefficient for a spherical particle of the same mass and anhydrous volume. In τ_0 it refers to the hydrated volume.

[a] All use Perrin's [42] solutions for the rotational frictional ratios for ellipsoids.

[b] There are two if the optical axis does not coincide with the geometric axis of ellipsoid of revolution. There are also two (θ_+) for general ellipsoids (see below).

[c] Three for ellipsoids of revolution, five for general ellipsoids.
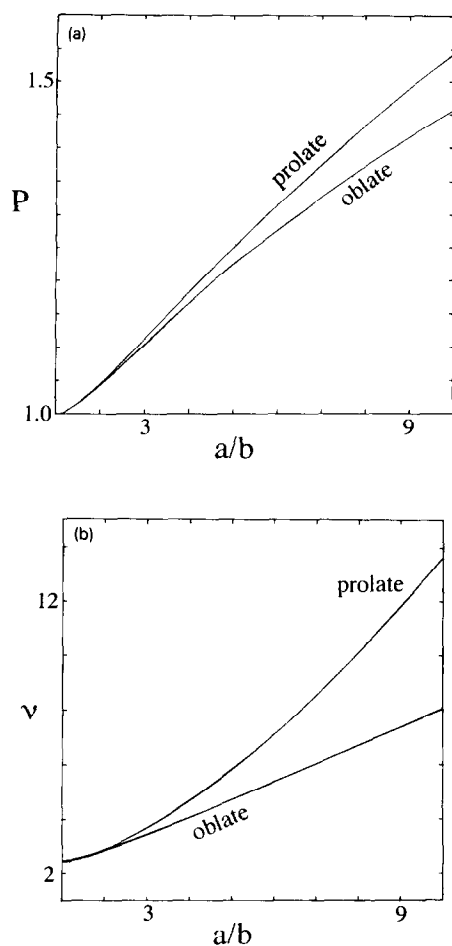
Fig. 3. Ellipsoid of revolution axial ratio (a/b). Plotted between $1 \le a/b \le 10$ for (a) the Perrin frictional ratio function P and (b) the viscosity increment ν. For the experimental evaluation of P or ν, an assumption concerning the hydration of the macromolecule is needed.

Insofar as parameters based on bulk solution properties are concerned, Simha [43] extended Jeffery's [44] earlier treatment for the viscous flow of solutions of ellipsoids of revolution to include the case of Brownian motion and gave an explicit relationship for the viscosity increment ν, defined by

$$\nu = [\eta]/v_s \qquad (6)$$

in terms of the semi axes a,b $(a \ge b)$ of these ellipsoids. Saito [45], using a different calculation procedure obtained the same result, suggesting that Simha had made an incorrect assumption (particles rotating with *zero* angular velocity) but had arrived

at the correct result by making an "error in calculation", a discrepancy resolved some 30 years later [46]. The dependence of ν on a/b calculated from the correct formula is shown graphically in Fig. 3b. The full formulae, containing elliptic integrals solvable using standard numerical packages [47] will not be given here since they are not much simpler than the equation for general triaxial ellipsoids given below. Simple approximations are available [43] for the limits of long axial ratios $(a \gg b)$ where prolate ellipsoids can be approximated by rods and oblate ellipsoids by discs:

$$\text{Rods: } \nu \sim \frac{(a/b)^2}{15(\ln(2a/b) - 1.5)}$$

$$+ \frac{(a/b)^2}{5(\ln(2a/b) - 0.5)} + \frac{14}{15}$$

$$\text{Disks: } \nu \sim \frac{16}{15}\tan^{-1}\left(\frac{a}{b}\right) \qquad (7)$$

with $(a/b) \gg 1$ in both cases. The molar covolume, U, which can be obtained from measurements of the thermodynamic non-ideality of solutions (using either osmometry, light scattering or sedimentation equilibrium measurements) has been worked out for ellipsoids of revolution [49,50,60]. Expressed in its reduced (dimensionless) form $(u_{red} = U/(N_A \cdot v_s))$:

$$u_{red} = 2 + \frac{3}{2}\left(\frac{1 + \sin^{-1}\epsilon}{\epsilon(1 - \epsilon^2)^{1/2}}\right)$$

$$\times \left(1 + \frac{1 - \epsilon^2}{2\epsilon}\ln\frac{1 + \epsilon}{1 - \epsilon}\right) \qquad (8)$$

where ϵ (the "ellipticity") $= (1 - (a^2/b^2))^{1/2}$, with $a/b \ge 1$. Eqs. (4), (7) and (8) are just the salient ellipsoid of revolution shape parameters. Others have been worked out based on rotational diffusion or radius of gyration measurements.

So in this way, a whole library of shape functions are available whose functional dependence on the axial ratio of the ellipsoid of revolution are known, and extensive tables have been given [28].

4.1. The hydration problem

An important problem in using the viscosity increment ν, the reduced molecular covolume u_{red}, the

Perrin frictional ratio function P, or related rotational diffusion shape parameters is that to obtain these from experimental parameters, knowledge of, or an assumption of the extent of hydration of the molecule is required, as represented by v_s, or equivalently the parameter w (also referred to by the parameter "δ" in some texts [48])

$$v_s = \bar{v} + w/\rho_0 \qquad (9)$$

w is the mass of solvent bound (chemically and physically entrapped) per unit mass of anhydrous macromolecule. Although hydration is a notoriously difficult parameter to measure with any meaningful precision, and largely depends on which technique is employed to measure it, a value of 0.3–0.35 g/g is often taken for proteins [48,53], which is approximately equivalent to a bound monolayer of surface water. Use of other shape functions summarised in Table 2 also requires "assumed" hydration values.

Perkins [25] has presented an algorithm for a more refined estimate of the protein hydration based on the amino acid composition of a protein. For polysaccharides and glycoproteins it can be much higher {e.g. 100 g/g for a mucin [53]}. Looking at things from a different direction, if a reasonable estimate for the axial ratio of the molecule is known from some other source (from e.g. crystallography, and assuming the axial ratio is approximately the same in dilute solution) the hydration can be calculated from the measured frictional ratios, and this has been done for a range of proteins by Squire and Himmel [54], where an average value for w of ca. 0.5 g/g can be inferred.

4.2. Hydration independent shape functions

A pair of shape functions can be combined together to eliminate the requirement for an estimate of w or v_s. The idea of combining analytically hydrodynamic shape functions dates back as long ago as 1953 with Scheraga and Mandelkern [55] who combined the relations of Perrin and Simha to give the well-used β function (Table 3), extending the original "graphical" approach of Oncley [56]. The β-function has proved, however, very insensitive to shape and has had most use as a quasi-constant parameter for determining molecular weights from intrinsic viscosity and sedimentation velocity data.

Rotational diffusion phenomena provide in general parameters which are more sensitive functions of shape than the corresponding translational ones but as stated above they come at a price in terms of difficulty of measurement. Several hydration independent functions can be generated by combination with either ν or P (such as κ_j or $\xi_j \cdot j = 1 - 5$) with the depolarisation anisotropy relaxation times [28]. Λ and Ψ are formed by combination of respectively ν and P with the harmonic mean rotational relaxation time. The Λ function, which can be measured without too much difficulty, is a particularly sensitive function of axial ratio and an example of its application can be found in Rholam and Nicolas [63] for neurophysin.

Another relatively recent development has been the use of compound shape functions involving molecular excluded volumes [60,62]. The molar covolume, U (ml $\cdot$ mol^{-1}) for a system of macro-

Table 3

"Compound" hydration independent shape parameters. Each formed by combining two of the shape functions (shown in parentheses) from Table 2

Shape parameter (as function of a/b)	Comment	Reference
$\beta(\nu, P)$	Very poor sensitivity to axial ratio and high sensitivity to experimental error	[55]
$\Psi(\tau_h/\tau_0, P)$	Very poor sensitivity to axial ratio and high sensitivity to experimental error	[58,59,28]
$\psi(u_{red}, P)$	Poor sensitivity to axial ratio and high sensitivity to experimental error	[60]
$R(\nu, P)$	Sensitive function for small axial ratios	[61,67]
$\Lambda(\tau_h/\tau_0, \nu)$	Very sensitive function, except at very low axial ratio ($a/b < 2.0$)	[57]
$\Pi(u_{red}, \nu)$	Sensitive function, except at very low axial ratio ($a/b < 2.0$)	[62]

molecules can be obtained from the thermodynamic second virial coefficient B (after correction for – or suppression of – charge effects). This covolume function is both a function of shape and hydration but can be "reduced" to give a function u_{red} of shape alone [62]. To experimentally measure it a value for the hydration is still required, but again, the latter can be eliminated by combination with either the Perrin frictional ratio to give the hydration independent parameter ψ [60] or with the viscosity increment ν to give the hydration independent Π function [62]. Although the ψ function is very insensitive to shape – and rather disappointingly so – the Π function on the other hand is quite sensitive for prolate ellipsoids, and appears to be one of the most useful of the "hydration independent" ellipsoid of revolution shape functions available.

Finally, another "hydration independent" parameter is the ratio $R = k_s / [\eta]$, where k_s is the sedimentation concentration dependence parameter from the limiting relation:

$$s_{20,w} = s_{20,w}^0 (1 - k_s c) \tag{10}$$

or for more concentration dependent systems

$$\frac{1}{s_{20,w}} = \frac{1}{s_{20,w}^0} (1 + k_s c) \tag{11}$$

where c is the concentration and $s_{20,w}^0$ is the infinite dilution sedimentation coefficient. Eq. (10) is usually a better fit for globular particles, Eq. (11) for asymmetric ones. It is known empirically [64–66] that $R \sim 1.6$ for spheroidal particles and < 1.6 for more asymmetric particles; after a number of assumptions and approximations, a simple relation between R, ν and P has been provided ([61], see also [67]).

It should be pointed out that there is a general difficulty faced with all the "hydration independent shape functions" presented in Table 3, namely that – and not surprisingly – they are not as sensitive to shape as their hydration dependent precursors, the β-function being probably the most extreme example. However three (Λ, Π and R) do appear particularly useful, at least for prolate ellipsoids (Fig. 4). Tables 4 and 5 give all these functions, together with ν, P and β for prolate and oblate ellipsoids in the range $1 \leq a/b \leq 100$. Eqs. analogous to (5a) and (5b) giving (a/b) directly in terms of ν, β, Λ, Π

and R will be available shortly [68]. A "QUICK-BASE" routine (ELLIPS 1) will also be made available.

5. The general triaxial ellipsoid

A comprehensive description of this type of modelling is given in Ref. [29]. For many macromolecules the ellipsoid of revolution model can apparently give a reasonable representation of the gross conformation of macromolecules in solution. Indeed examination of the axial dimensions of macromolecules in crystal form [83] reveals that for many proteins, two of the three dimensions are approximately equal. Their are, however, two serious drawbacks: (1) a decision has to be made a priori between the two types of ellipsoid (viz. prolate and oblate). Virtually all of the usable hydration independent shape functions do not distinguish between the two (viz. they are not single-valued); (2) there are many classes of macromolecule which lie intermediate between a prolate shape (one long axis, two short) and an oblate shape (two long axes, one short). As a result, hydrodynamicists have for a long time recognised the advantages of having a model which does not have this restriction of two equal axes: the general triaxial ellipsoid (semi-axes $a \geq b \geq c$). This caters for a much wider range of shapes, from discs ($a = b \gg c$), rods ($a \gg b = c$), tapes ($a \gg b \gg c$) and all intermediary shapes (Fig. 5).

The reason the general ellipsoid has not been available until relatively recently has been that the relation between the shape functions and the two axial ratios which characterise a general ellipsoid had either not been worked out (e.g. ν, u_{red}) or they were computationally unavailable, i.e. unavailability of satisfactory numerical routines – without convergence problems – for the evaluation of the elliptic type of integrals involved [29]. Over the last twenty years both of these problems have largely been addressed. Small and Isenberg [69] demonstrated that the Perrin elliptic integrals could be solved numerically using fast mainframe computers to evaluate the rotational and translational frictional ratio functions. The subsequent availability of the viscosity increment ν both numerically [70] and then analytically [71,72] together with the reduced molecular volume
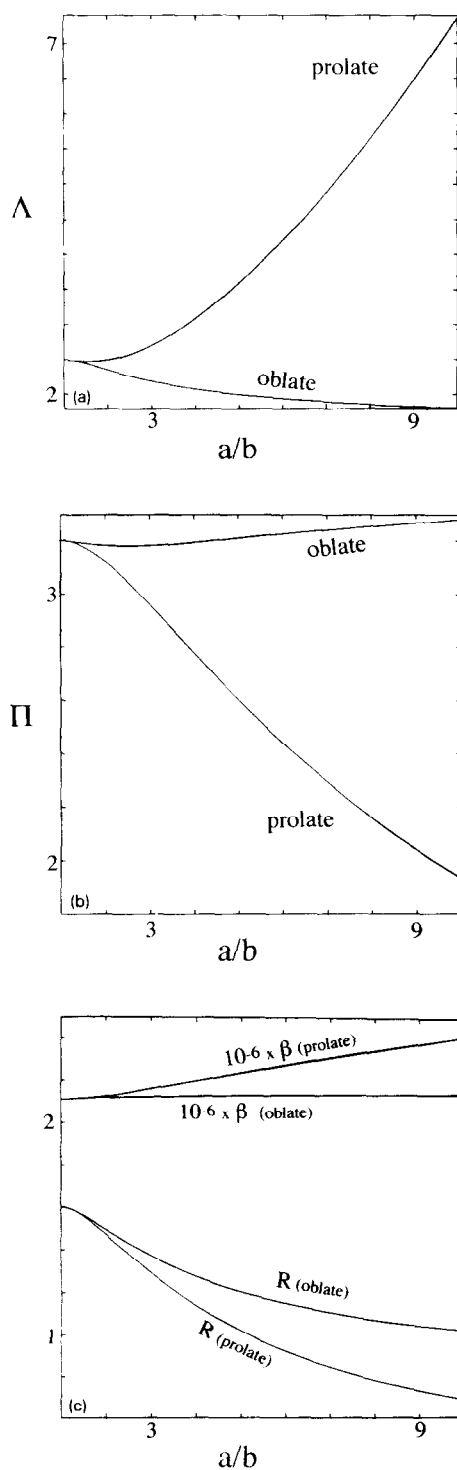
Table 4

Values of P, ν, Λ, Π, R and β as a function of axial ratio for prolate ellipsoids of revolution

a/b (prolate)	P	ν	Λ	Π	R	$10^{-6} \times \beta$
1	1.000	2.500	2.500	3.200	1.600	2.112
2	1.044	2.908	2.490	3.122	1.471	2.127
3	1.113	3.685	2.692	2.960	1.291	2.160
4	1.183	4.663	3.071	2.778	1.138	2.198
5	1.250	5.806	3.575	2.601	1.017	2.237
6	1.314	7.099	4.177	2.438	0.921	2.275
7	1.375	8.533	4.862	2.291	0.844	2.312
8	1.434	10.103	5.624	2.159	0.782	2.346
9	1.490	11.804	6.457	2.041	0.730	2.378
10	1.543	13.634	7.359	1.935	0.686	2.408
20	1.996	38.530	19.749	1.288	0.465	2.632
30	2.359	74.506	37.720	0.980	0.379	2.776
40	2.671	120.765	60.841	0.799	0.332	2.880
50	2.950	176.812	88.599	0.679	0.302	2.960
60	3.205	242.289	121.594	0.593	0.280	3.027
70	3.442	316.923	158.908	0.527	0.264	3.082
80	3.664	400.495	200.692	0.476	0.251	3.130
90	3.874	492.822	246.855	0.435	0.240	3.173
100	4.074	593.751	297.318	0.400	0.231	3.210

u_{red} for general "tri-axial" ellipsoids [73], has now meant that a virtually complete set of hydration independent triaxial shape parameters are now available and Table 6 gives all the principle hydration dependent and independent shape functions, together with their relation to experimental parameters. Ref. [29] shows how all these parameters can be coded up in terms of the axial ratios $(a/b, b/c)$ or equivalently the (a,b,c) (the absolute values of (a,b,c) do not matter, what is important is the value of the two ratios $(a/b, b/c)$ they define). In Table 6, U is the molar covolume (ml/mol) and V is the (hydrated) volume (ml) of the macromolecule, related to the hydrated specific volume (ml/g) by

$$V = v_s \cdot M/N_A \tag{12}$$

M is the molecular weight or molar mass (g/mol) and N_A is Avogadro's number (mol^{-1}). θ_+, θ

Fig. 4. Hydration independent shape functions. Plotted as a function of axial ratio for prolate ellipsoids, between $1 \le a/b \le 10$. Only the three most sensitive (Λ, Π and R) together with β are shown. (a) Λ; (b) Π; (c) R and β.

Table 5
Values of P, ν, Λ, Π, R and β as a function of axial ratio for oblate ellipsoids of revolution

a/b (oblate)	P	ν	Λ	Π	R	$10^{-6} \times \beta$
1	1.000	2.500	2.500	3.200	1.600	2.112
2	1.042	2.854	2.356	3.180	1.494	2.118
3	1.105	3.431	2.187	3.179	1.369	2.124
4	1.166	4.059	2.070	3.192	1.274	2.128
5	1.224	4.708	1.989	3.208	1.203	2.131
6	1.277	5.367	1.931	3.225	1.148	2.134
7	1.327	6.032	1.887	3.241	1.105	2.135
8	1.373	6.700	1.854	3.255	1.071	2.137
9	1.417	7.371	1.827	3.268	1.043	2.138
10	1.458	8.043	1.805	3.280	1.019	2.139
20	1.783	14.804	1.705	3.352	0.901	2.143
30	2.020	21.585	1.670	3.384	0.856	2.145
40	2.212	28.370	1.653	3.403	0.833	2.145
50	2.375	35.158	1.642	3.415	0.819	2.146
60	2.519	41.946	1.635	3.423	0.810	2.146
70	2.648	48.736	1.630	3.429	0.803	2.147
80	2.765	55.525	1.627	3.434	0.798	2.147
90	2.873	62.315	1.624	3.437	0.793	2.147
100	2.974	69.104	1.621	3.441	0.790	2.147

(s^{-1}) are the electric birefringence decay constants {two for a monodisperse solution of triaxial ellipsoids} [18,81] and R_g is the radius of gyration (cm). $f(Z,I)$ is a function of macromolecular charge Z and solution ionic strength, I. $f \to 0$ at the isoelectric pH for proteins, and as I is increased. To an approximation [49]

$$f(Z,I) \approx Z^2/2I \qquad (13)$$

A better approximation has been given by Wills et al. [82]. In the expression for ν, δ is a small term (less than 1% of the rest) given by:

$$\delta = -\frac{1}{5abc}$$

$$\times \left[\frac{\left(\dfrac{a^2 - b^2}{a^2\alpha_1 + b^2\alpha_2} + \dfrac{b^2 - c^2}{b^2\alpha_2 + c^2\alpha_3} + \dfrac{c^2 - a^2}{c^2\alpha_3 + a^2\alpha_1} \right)^2}{\left(\dfrac{a^2 + b^2}{a^2\alpha_1 + b^2\alpha_2} + \dfrac{b^2 + c^2}{b^2\alpha_2 + c^2\alpha_3} + \dfrac{c^2 + a^2}{c^2\alpha_3 + a^2\alpha_1} \right)} \right]$$

$$(14)$$

and in the equation for the reduced decay constants $\theta_{\pm}^{red}$, the terms Q_a, Q_b and Q_c are given by

$$Q_a = \frac{b^2 + c^2}{b^2\alpha_2 + c^2\alpha_3}, \quad Q_b = \frac{c^2 + a^2}{c^2\alpha_3 + a^2\alpha_1},$$

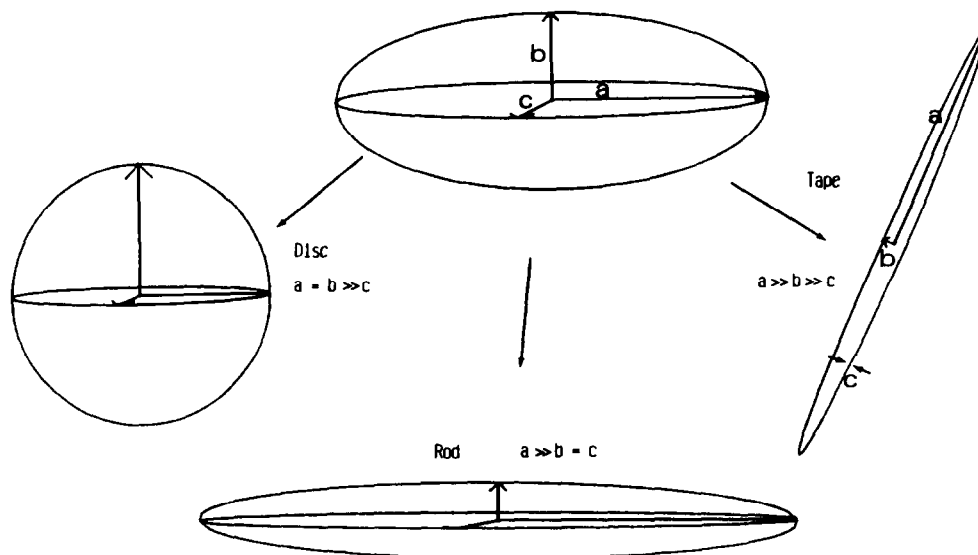$$Q_c = \frac{a^2 + b^2}{a^2\alpha_1 + b^2\alpha_2} \qquad (15)$$

Fig. 5. The general triaxial ellipsoid (semi-axes $a > b > c$) and its extremes (disc, rod and tape). From [29].

All of the shape functions (apart from the radius of gyration based function G) require for their evaluation one or more of the following elliptic type of integrals:

$$\alpha_1 = \int_0^\infty \frac{d\lambda}{(a^2 + \lambda)\Delta} \; ; \; \alpha_2 = \int_0^\infty \frac{d\lambda}{(b^2 + \lambda)\Delta}$$

$$\alpha_3 = \int_0^\infty \frac{d\lambda}{(c^2 + \lambda)\Delta}$$

$$\alpha_4 = \int_0^\infty \frac{d\lambda}{(b^2 + \lambda)(c^2 + \lambda)\Delta}$$

$$\alpha_5 = \int_0^\infty \frac{d\lambda}{(c^2 + \lambda)(a^2 + \lambda)\Delta}$$

$$\alpha_6 = \int_0^\infty \frac{d\lambda}{(a^2 + \lambda)(b^2 + \lambda)\Delta}$$

$$\alpha_7 = \int_0^\infty \frac{\lambda d\lambda}{(b^2 + \lambda)(c^2 + \lambda)\Delta}$$

$$\alpha_8 = \int_0^\infty \frac{\lambda d\lambda}{(c^2 + \lambda)(a^2 + \lambda)\Delta}$$

$$\alpha_9 = \int_0^\infty \frac{\lambda d\lambda}{(a^2 + \lambda)(b^2 + \lambda)\Delta}$$

$$\alpha_{10} = \int_0^\infty \frac{d\lambda}{\Delta} \tag{16}$$

Table 6
Shape functions for general triaxial ellipsoids. Parameters marked with an asterisk require an estimate for the hydration of the macromolecule for their experimental measurement. Only the most significant ones shown (others can be found in Ref. [28])

Parameter	Formulation	Relation to experimental parameters	Reference
* ν	$\frac{1}{abc}\left\{\frac{4(\alpha_7 + \alpha_8 + \alpha_9)}{15(\alpha_8\alpha_9 + \alpha_9\alpha_7 + \alpha_7\alpha_8)}\right.$ $+ \frac{1}{5}\left[\frac{\alpha_2 + \alpha_3}{\alpha_4(b^2\alpha_2 + c^2\alpha_3)}\right.$ $+ \frac{\alpha_3 + \alpha_1}{\alpha_5(c^2\alpha_3 + a^2\alpha_1)}$ $\left.\left.+ \frac{\alpha_1 + \alpha_2}{\alpha_6(a^2\alpha_1 + b^2\alpha_2)}\right]\right\} + \delta$	$Eq.$ (6)	[71,72,28,74]
* P	$2/(abc)^{1/3}/\alpha_{10}$	Eqs. (1–3)	[38,69,28]
* u_{red}	$2 + \left(\frac{3}{2\pi abc}\right)R.S$	$\frac{U}{N_A V} \equiv \frac{1}{N_A V}$ $(2BM^2 - f(Z,I))$	[73]
* τ_h / τ_0	$1/[a^2\alpha_1 + b^2\alpha_2 + c^2\alpha_3]$	$(kT\tau_h)/3\eta_0 V)$	[75,28]
* θ_+^{red}	$\frac{abc}{12}\left\{\left(\frac{1}{Q_a} + \frac{1}{Q_b} + \frac{1}{Q_c}\right)\right.$ $\pm\left[\left(\frac{1}{Q_a^2} + \frac{1}{Q_b^2} + \frac{1}{Q_c^2}\right)\right.$ $-\left(\frac{1}{Q_a Q_b} + \frac{1}{Q_b Q_c}\right.$ $\left.\left.\left.+ \frac{1}{Q_c Q_a}\right)\right]^{1/2}\right\}$	$(\eta_0/kT) \cdot V \cdot \theta_+$	[18,76,77,28,78]
β	$(N_A^{1/3}/16200\pi^2)^{1/3} \cdot (\nu^{1/3}/P)$	$N_A s[\eta]^{1/3}\eta_0/(M^{2/3}(1 - \bar{v}\rho_0)100^{1/3})$	[56,79,28]
Π	u_{red}/ν	$U/([\eta] \cdot M) \equiv (2BM/[\eta]) - f(Z, I)/([\eta]M)$	[80]
G	$(1/5)(a^2 + b^2 + c^2)/(abc)^{2/3}$	$((4\pi N_A)/(3\bar{v}M))^{2/3}R_g^2$	[80]
Λ	$\nu/(\tau_h/\tau_0)$	$(3\eta_0[\eta]M_r)/(N_A kT\rho_h)$	[75]
R	$2(1 + P^3)/\nu$	$k_s/[\eta]$	[83]
δ_+	$60\theta_\pm^{red}\nu$	$(6\eta_0/N_A kT) \cdot [\eta] \cdot M \cdot \theta_\pm$	[83]

where

$$\Delta = \left((a^2 + \lambda)(b^2 + \lambda)(c^2 + \lambda) \right)^{1/2} \qquad (16a)$$

and λ is a dummy variable. For an ellipsoid of revolution, simply set $c = b$ (prolate) or $c = a$ (oblate).

The formulation for u_{red} requires the numerical evaluation of two double integrals of the type:

$$R = \frac{2}{3\pi} \int_0^{\pi/2} \int_0^{\pi/2} \cos u \; du \; dv$$

$$\times \left\{ \left(\frac{a}{bc} + \frac{b}{ac} + \frac{c}{ab} \right) \Delta^2 \right.$$

$$- \sin^2 v \cos^2 v \cos^2 u \; \Delta^4 \left(\frac{1}{a^2} - \frac{1}{b^2} \right) \frac{1}{c} \left(\frac{b}{a} - \frac{a}{b} \right)$$

$$- \sin^2 u \cos^2 u \; \Delta^4 \left(\frac{\cos^2 v}{a^2} + \frac{\sin^2 v}{b^2} - \frac{1}{c^2} \right)$$

$$\cdot \left[\frac{1}{c} \left(\frac{b \cos^2 v}{a} + \frac{a \sin^2 v}{b} \right) \right.$$

$$\left. \left. + \frac{c}{ab} - \frac{b}{ac} - \frac{a}{bc} \right] \right\} \qquad (17a)$$

$$S = \frac{8}{3} \int_0^{\pi/2} \int_0^{\pi/2} \cos u \; du \; dv$$

$$\times \left\{ \left(\frac{bc}{a} + \frac{ca}{b} + \frac{ab}{c} \right) \Delta \right.$$

$$- \sin^2 v \cos^2 v \cos^2 u \; \Delta^3 \, c \left(\frac{b}{a} - \frac{a}{b} \right)$$

$$\times \left(\frac{1}{a^2} - \frac{1}{b^2} \right)$$

$$- \sin^2 u \cos^2 u \; \Delta^3 \left(\frac{\cos^2 v}{a^2} + \frac{\sin^2 v}{b^2} - \frac{1}{c^2} \right)$$

$$\left. \cdot \left[c \left(\frac{b \cos^2 v}{a} + \frac{a \sin^2 v}{b} \right) - \frac{ab}{c} \right] \right\} \qquad (17b)$$

where

$$\Delta^{-2} = \frac{\cos^2 u \cos^2 v}{a^2} + \frac{\cos^2 u \sin^2 v}{b^2} + \frac{\sin^2 u}{c^2} \qquad (17c)$$

and again, for a prolate ellipsoid simply set $c = b$ and for an oblate, set $c = a$. All the integrals in Eqs. (16) and (17) can be readily solved numerically without convergence problems using standard computational packages, such as the NAG [47] routine D01AGF. A FORTRAN routine has been available for some time [78] incorporating these packages for evaluating the set of hydrodynamic parameters for a particle for any given value of its axial dimensions. We are on the verge of getting this mainframe routine, modified to include the covolume related functions (u_{red}, Π), downloaded onto PC. The reverse route – calculating $(a/b, \; b/c)$ or – if v_s is also known – (a,b,c), is not so easy: there is no analytical way of inverting the relations to give $(a/b, \; b/c)$ or (a,b,c) explicitly. Instead graphical methods have to be used.

5.1. Line solutions: the graphical intersection approach

All the triaxial ellipsoid shape functions share the common property of having a line solution of possible values for the axial ratios $(a/b, \; b/c)$ for any given value of the hydrodynamic function. A unique solution for these two axial ratios can be found from the intersection of two or more of these "line solutions", and Fig. 6 illustrates two line solutions for ν and P for a hypothetical ellipsoid particle of $(a/b, \; b/c) = (2.0, \; 2.0)$. A value of $(2.0, \; 2.0)$ is reproduced
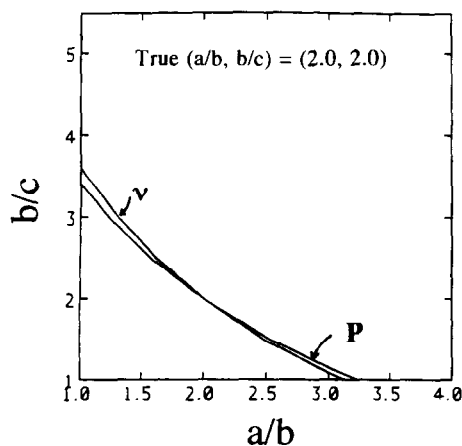

Fig. 6. Plots of constant values for ν and P in the $(a/b, \; b/c)$ plane corresponding to an $(a/b, \; b/c) = (2.0, \; 2.0)$. From [83].

Table 7

Comparison of graphical intersection properties of hydration independent triaxial ellipsoid shape functions

	Λ [a]	G [b]	δ_+ [c]	R [d]
Π	Poor intersection	Good intersection at high axial ratios	Good intersection at high axial ratios	NE
Λ		Good intersection at all axial ratios	NE	Good intersection at all axial ratios
G			Good intersection at low axial ratios	NE
δ_+				Good intersection at low ratios

[a] Assumes no internal rotation of chromophore or segmental rotation.

[b] From radius of gyration measurements (x-ray scattering or light scattering).

[c] Involves resolution of a two-term exponential decay.

[d] Some approximations concerning concentration dependence of sedimentation coefficients (k_s). NE: not examined.

from the intersection – but only just. Evidently this represents a very poor combination of functions, because of the shallowness of the intersection and their dependence on assumed values for hydration. To use the triaxial ellipsoid we have to find two

suitable shape functions that are (1) hydration independent, (2) experimentally measurable to a reasonable precision, (3) are sensitive to shape (and insensitive to experimental error) and (4) give a reasonable intersection (i.e. as orthogonal as possible). These
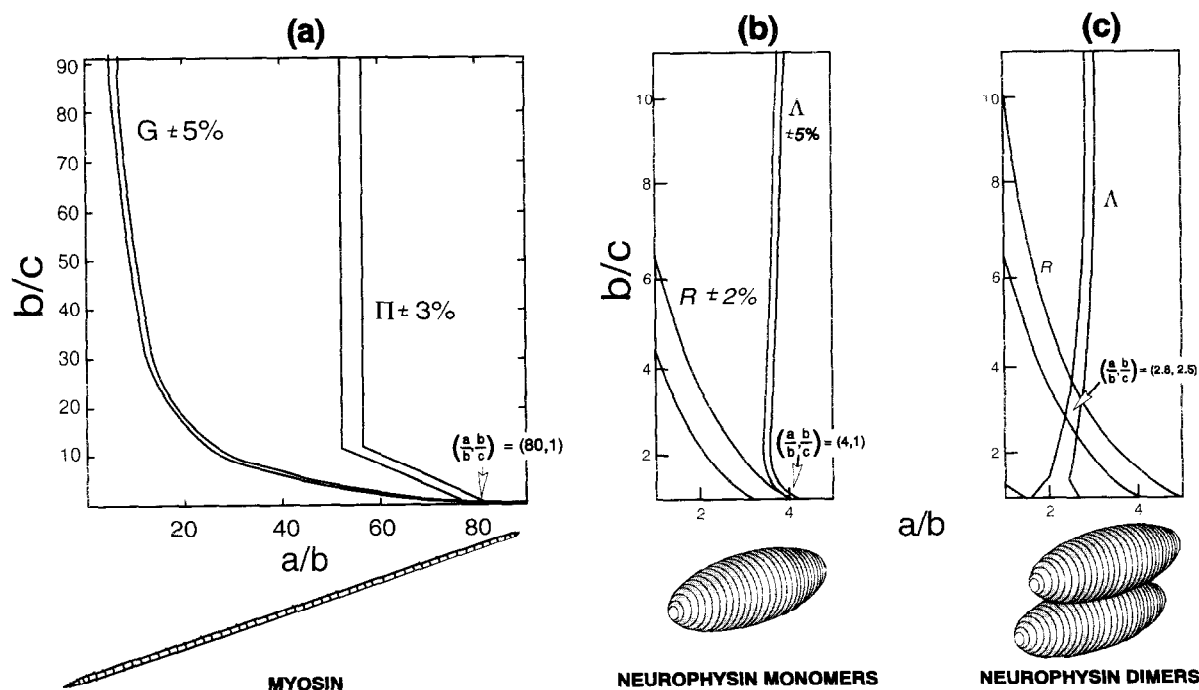

Fig. 7. Triaxial ellipsoid gross conformation evaluations for (a) myosin, (b) neurophysin monomers and (c) neurophysin dimers. (a) Plots of constant values for Π and G in the (a/b, b/c) plane for myosin and gross conformation predicted. From [80]. (b) Plots of constant values for Λ and R for neurophysin monomers [75]. (c) As (b) but for neurophysin dimers [75].

criteria are quite restrictive, and in Table 7 we have summarised the intersection properties between the most useful functions.

In choosing two suitable hydration independent functions we try to avoid where possible those requiring measurement of rotational diffusion or relaxation parameters because of the problems mentioned above of multi-exponential resolution [84,85] or deconvolution of source functions referred to above, together with further problems of internal rotations within the macromolecule in relation to the position of the chromophore. All these difficulties are further discussed in Ref. [29]. Electric birefringence (or dichroism) decay is, however, an attractive option not only because of the important advances in instrumentation referred to above but also because for ellipsoids there are only two exponentials to resolve. Resolving just two exponentials can be, however, still very difficult, especially where, for globular types of particle, the relaxation times are close together (see e.g., Ref. [28] for a comprehensive survey of the methods available, or Refs. [9,10] for the analogous situation with the dynamic light scattering of polydisperse systems) although the use of constrained procedures using another triaxial ellipsoid shape function – such as R or G – considerably improves the situation [29].

Fortunately, shape function combinations are now available which largely avoid the difficulties referred to above and three examples of applications are given in Fig. 7. In Fig. 7a the Π and G functions have been used to model the triaxial shape of myosin. Nonewithstanding the difficulties of modelling an ellipsoid to a particle that in reality has a "lop-sided" end, the result of $(a/b, b/c) = (80, 1)$ is in good agreement with predicted results from electron microscopy, and would appear to suggest that local variations in particle shape (principally in the case of myosin the S1 heads) or flexibility (the HMM/LMM interface) do not seriously distort estimates for the gross conformation of the molecule using the tri-axial ellipsoid in this way.

Some comment needs to be made on use of the G function, which comes from light scattering or solution X-ray scattering measurements, especially in terms of interpretation of the volume of the particle it refers to. To evaluate G experimentally a value for V the volume of the particle has to be assigned

(Table 6), and a decision has to be made whether this should refer to the anhydrous molecule or the solvated molecule. Insofar as surface water is concerned, only water whose density is different from bulk water will influence the scattering, so to an approximation if the hydration is due only to surface water then the G refers to the anhydrous particle. Grossmann et al. [87] have for example shown that low angle X-ray scattering "sees" only a hydration w of ca. 0.12 g/g for nitrite reductase. If, however, the effect of the interaction with water is to swell the molecule appreciably (as for e.g. mucus glycoproteins and other glycoconjugates [53,88]), then the swollen volume would be more appropriate: so some caution has to be expressed when applying G in this way.

For the modelling of globular particles at low axial ratio (one axial < 5) the intersection of G with Π is poor largely through insensitivity of the Π function in this region, and it is necessary to consider the use of other combinations of hydration independent shape functions. Other combinations considered (see [29,89]) have for example involved the $\delta_{\pm}$ functions (obtained from the electric birefringence or dichroism decay constants $\theta_{\pm}$ and extracted using a constrained non-linear least squares procedure). However, probably the best example so-far is a combination of the Λ function with the R function. Λ [57] requires the measurement of the intrinsic viscosity and the harmonic mean rotation relaxation time, τ_h, a parameter which can be obtained from steady state fluorescence depolarisation measurements without the need for multi-exponential resolution. Unlike Π-G, the Λ-R combination provides a sensitive intersection at low axial ratio, and has been used to provide us with an indication of the likely mode of association of monomers of the CNS protein neurophysin into dimers (Fig. 7b,c) [75]. Again, as for the myosin example above, despite the extra degree of freedom the general ellipsoid allows, the monomer still appears as a prolate model with two axes approximately equal $(a/b, b/c) \approx (4.0, 1.0)$. For the dimer this reduces to an overall $(a/b, b/c)$ of ca. $(2.8, 2.5)$ and the data therefore supports observations made earlier using ellipsoid of revolution models [63] that the association process is of a side-by-side rather than an end-to-end or other assembly.

5.2. Computer programmes

Three FORTRAN programmes for ellipsoid modelling have been available for some time: The first, now called "ELLIPS2" [78] evaluates the set of hydrodynamic parameters for any specified values of the semi axes ($a > b > c$) or alternatively the semi axial ratios (a/b, b/c), now updated to incorporate the Π and G functions. It can of course do the job also for ellipsoids of revolution, simply by setting $c = b$ (prolate ellipsoids) or c = a (oblate ellipsoids).

The second and third, now called "ELLIPS3" and "ELLIPS4", respectively [90], do the reverse procedure. For specified hydrodynamic parameters, the (a/b, b/c) can be evaluated from the graphical intersection of line solutions in the (a/b, b/c) plane. ELLIPS3 uses a simple intersection procedure involving the R and Λ functions (used for the neurophysin example mentioned above). This has now been updated to allow other combinations such as Π-G used for the myosin example. ELLIPS4 is a more complex routine in which the R function is combined with the electric birefringence decay time derived $\delta_{\pm}$ functions, but with the R-function used as a constraining function in the extraction of the decay constants – and greatly facilitating the extraction. This has also been updated to allow Π [89] or G [29] as the constraining functions.

All these programmes (ELLIPS2, ELLIPS3, ELLIPS4), currently in FORTRAN on the mainframe IBM 3081/Q at the University of Cambridge, are being downloaded into readily available PC form.

6. Bead modelling

A comprehensive description of this type of modelling can be found in Garcia de la Torre [30] or more recently in Garcia de la Torre [31]. There are many classes of macromolecule that cannot be reasonably represented by either ellipsoid of revolution or triaxial ellipsoid models. Examples include antibodies and the complement system, T-even bacteriophages and DNA complexes. Bloomfield et al. [91] took on an older idea of Kirkwood [92] to calculate the hydrodynamic properties of particles by modelling them as an array of spherical beads which
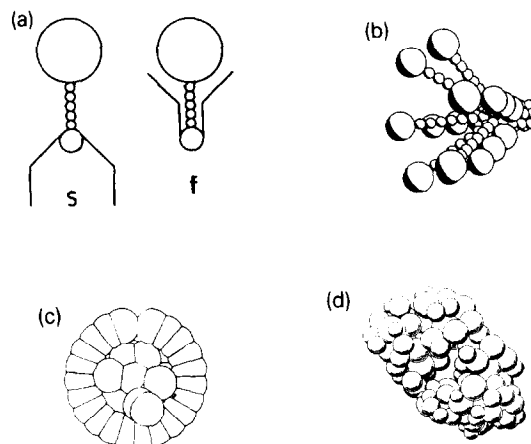
Fig. 8. Examples of bead models. (a) T-even bacteriophage in slow (s) and fast (f) forms ($s_{20,w}^{0}$ ~ 710S and 1020S, respectively). Modelled on sedimentation and diffusion coefficient data. From [93] and [30]. (b) Cyclic AMP receptor associated with 80 base-pair DNA. Only maximum bending of the DNA reproduces the measured rotational diffusion decay constant (from electric dichroism decay). From [94] and [95]. (c) C1 complex from the complement system. Modelled on sedimentation coefficient and R_g data. From [96]. (d) Fab'' fragment of a chimeric antibody. Modelled on sedimentation coefficient and R_g data. From [97].

interact in a way described by the Burgers–Oseen interaction tensor for spheres: in this way, and using an approximate "double sum" formula method the diffusion coefficient or sedimentation coefficient could be calculated for a given model [91]. The theory was subsequently extended to permit the evaluation of the rotational diffusion relaxation times, the fluorescence depolarisation anisotropy relaxation times τ_i ($i = 1$–5), the radius of gyration (assuming uniform density) and the intrinsic viscosity. Examples of bead models evaluated using this procedure are given in Fig. 8.

6.1. Principle

The idea is to combine the well known hydrodynamic properties of rigid spheres and interaction tensors describing arrays of spheres to estimate the hydrodynamic properties for a given structure. The spherical elements may correspond to real subunits in the assembly see, e.g., [98], although this is not necessarily the case [31]. In this way very sophisti-

cated and beautiful representations of conformation can be given, as shown in Fig 8. Either:

(i) the set of hydrodynamic parameters is calculated for a given model and then compared with the actual measured values. The model is then successively iterated (after adequate allowance for hydration) until acceptable agreement is obtained or,

(ii) the set of hydrodynamic parameters is calculated for two or more plausible models for a structure and the one giving closest agreement with the experimental data is chosen.

An obvious complication arises with (i), in that although once good agreement between the calculated and experimental parameters has been obtained for a certain model, there is no reason not to suppose that a whole series of other models give the same agreement – this "uniqueness problem" becomes more acute the more sophisticated the models are, although the problems are lessened the more the number of independent hydrodynamic parameters are used. In practice (i) needs a good starting estimate for the structure, based on for example X-ray crystallography. For example, in their modelling of antibody structures, Gregory et al. [99] used the known crystal coordinates of a hingeless mutant antibody known as "Dob" or "McG" and evaluated the structures of other antibodies by comparing the $(s_{20,w}^0, R_g)$ datasets of each antibody with the $(s_{20,w}^0, R_g)$ for Dob. A similar approach was adopted by Morgan et al. [97] for modelling the murine Fab fragment from the chimareric antibody B72.3 (Fig. 8d) This work [99,97] together with more recent studies [100,101] has clearly shown that antibodies are not planar structures as often depicted in textbooks, but are folded, bent structures: Fig. 9 gives two views of a chimeric antibody demonstrating this.

With (ii) however, Perkins [96] compared the $(s_{20,w}^0, R_g)$ datasets for plausible models of a variety of complement factors with the measured $(s_{20,w}^0, R_g)$ to select the best model in each case. A similar approach, by modelling the low-angle X-ray scattering data directly, demonstrating a "trigonal antiprism" structure for the assembly of 11S rapeseed globulin subunits has been given by Plietz et al. [98]. Porschke and Antosiewicz [94,95] have adopted a similar strategy using electro-optic measurements for selecting the best model for the binding of the cAMP
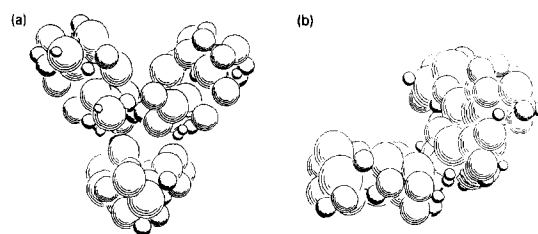

Fig. 9. (a) Front and (b) side views of the bead model of the chimeric IgG antibody cB72.3 demonstrating a clear non-planar structure. A hydration, w, of 0.25 g/g was used. Modelled on sedimentation coefficient and R_g data [100,101].

receptor to an 80 base-pair DNA fragment. Only a model of maximum bending of the DNA wrapping around the protein (Fig. 8c) reproduces the measured electric dichroism decay constant data on the basis of electric dichroism decay times.

As with ellipsoid modelling (also referred to as the "whole-body" approach [29]), hydration has to be dealt with. A value of 0.35 g H_2O/g protein for w has been commonly taken [25] or in, e.g. Gregory et al.'s [99] work, the hydration for a mutant antibody with known crystal coordinates was assumed to be the same as the other antibody classes modelled.

6.2. Reduced units and P, ν, G

Instead of working with P, $ν$, G etc., in his bead model computer programme "TRV" and the earlier programmes Garcia de la Torre [30] worked with "reduced" parameters which were essentially equivalent to P, $ν$ and G, etc. In order to try and get some consistency between the ellipsoid and bead approaches, Byron [100] has adapted TRV to permit the use of P, $ν$, G, etc. From these, if estimates of the specific volume (hydrated or otherwise) are known, the predicted sedimentation coefficients, intrinsic viscosities, gyration radii, rotational relaxation times etc. can be given.

6.3. Rigorous and approximate methods

This is a very brief summary of the theory given in Garcia de la Torre [30,31]. Consider first of all the translational frictional properties. Each bead in a given model is assigned the Stokes-law friction coefficient of

$$\zeta_i = 6\pi\eta_0\sigma_i \ (i = 1,\ldots\ldots N) \tag{18}$$

where σ_i is the bead radius, which does not have to be constant from bead to bead. For an assembly of beads moving with velocity u_i in a fluid at rest, the force on the solvent exerted by the array of beads is given by

$$F_i = \zeta_i u_i - \sum_i T_{ij} F_j \quad i,j = 1,2,...,N; \; j \neq i \qquad (19)$$

where, T_{ij} is the hydrodynamic interaction tensor as modified by Garcia de la Torre and Bloomfield [102,103]. For the particular case of sedimentation velocity the u_i equal the velocity of sedimentation. Similar representations are available for the intrinsic viscosity and the five rotational relaxation times (τ_i, $i = 1-5$).

For most applications evaluation of the full interaction tensor in Eq. (19) is not necessary, and instead the so-called "double sum" over pairwise contributions from the model's beads is normally sufficient. One such double sum, for the frictional coefficient is [91]

$$f = \frac{\sum_i \zeta_i}{1 + \left(6\pi\eta \sum_i \zeta_i\right)^{-1} \sum_{i,j} \zeta_i \zeta_j R_{ij}^{-1}} \quad i,j = 1,...,n; \; i \neq j$$

$$\qquad (20)$$

where R_{ij} is the distance between the bead centres. Similar double sum formulae exist for rotational relaxation times [104] and the intrinsic viscosity [105], with the simplest approximation for the latter being given by [106]:

$$[\eta] = \frac{5N_A V}{2M} + \frac{N_A \pi}{M} \left(\sum_i \sigma_i r_i^2\right)^2$$

$$\times \left(\sum_i \sigma_i r_i^2 + \sum\sum_{i \neq j} \sigma_i \sigma_j R_{ij}^{-1} R_i \cdot R_j\right)^{-1} \quad (21)$$

where r_i is the position vector of a bead from the viscosity centre.

All these approximate formula save considerably on computer time, but can contribute to error. The increasing availability of computing power has however made the use of approximate formulae such as Eqs. (20) and (21) largely redundant (in much the

same way that the availability of routines for solving elliptic integrals has made approximate equations for ellipsoids of revolution redundant with "whole body" modelling). The full rigorous method, largely developed by Garcia de la Torre and Bloomfield [103,107,108], is now fully accessible. For example, the frictional coefficient from specified coordinates for a bead model can be calculated using the formula

$$f = \frac{1}{3} Tr\left\{\sum_{ij} C_{ij}\right\} \qquad (22)$$

where Tr indicates the sum of the diagonal elements of a tensor and the C_{ij} are the blocks of the inverse matrix $C = B^{-1}$. B in turn is the matrix of coefficients of the tensor B_{ij} in the expression

$$\sum_i B_{ij} F_j = \zeta_i u_i \qquad (23)$$

with the $B_{ii} = 1$ and $B_{ij} = T_{ij}$ when $i = j$. Once f has been evaluated for a given set of bead coordinates then the Perrin parameter P can be specified, and if the hydration etc. is specified the sedimentation coefficient and diffusion coefficients can be evaluated as usual. Similar procedures are available for the prediction of the other hydrodynamic properties (see e.g. [30]).

6.4. Shell models

A form of bead modelling was proposed during the early developments of bead theory [91] which modelled the whole surface of the particle by an array of very small spherical beads. This "shell model" approach has been applied to a whole variety of shapes [109–113].

6.5. Computer programmes

The bead modelling routine TRV (replacing earlier versions known as GENDIA and GENTRA) is given in Garcia de la Torre [29], and some typical output for the antibody IgG3 is given in Ref. [31]. A further modified version, permitting prediction of P, ν and G directly (cf, Table 7 for ellipsoids) has been given in Byron [100].

7. General particle shapes

Both ellipsoid modelling and bead modelling require stringent assumptions concerning the monodispersity of the macromolecular system being represented. This discounts molecules like polysaccharides and related glycopolymers such as mucus glycoproteins (although for fairly rigid systems thereof ellipsoidal axial ratios can still be applied in a loose sort of way). For polydisperse types of molecules such as these we have to use hydrodynamics in a general sort of way using what are known as the Mark–Houwink–Kuhn–Sakurada coefficients [86] and the Wales–van Holde ratio, $k_s/[\eta]$ ($=R$) [116,33,66,67] to distinguish between classes of particle conformation (between the three extremes of compact sphere, rigid rod and random coil).

7.1. Mark–Houwink–Kuhn–Sakurada (MHKS) coefficients

The dependence of a hydrodynamic parameter on the molecular weight for a homologous series of fractions for a macromolecule gives a coefficient which will be a measure of the shape of the macromolecule. There are several such coefficients [86,32,33]:

$$[\eta] = K' \cdot M^a \tag{24}$$

$$s^0_{20,w} = K'' \cdot M^b \tag{25}$$

$$D^0_{20,w} = K''' \cdot M^{-\epsilon} \tag{26}$$

$$R_g = K'''' \cdot M^c \tag{27}$$

The superscript in Eq. (25) is sometimes given as $1 - b$ [67], and c in Eq. (27) is sometimes given as ν [113a]. The exponent coefficients a,b, ϵ and c will all depend on the conformation of the particle (Table 8), and are extracted usually from double-logarithmic plots (see e.g., Fig. 10). The homologous series can be obtained by for example fractionation using gel filtration or sonication procedures. To give two examples, a range of coefficients (b, ϵ and c) have been applied by Sheehan and Carlstedt [114,115] and Jamieson et al. [115a] to mucin glycoproteins, demonstrating that these molecules have random-coil like properties in solution, and the a,b coefficients have been applied to the polyanionic polysaccharide

Table 8
Mark–Houwink–Kuhn–Sakurada (MHKS) coefficients and $k_s/[\eta]$

Conformation	a	b	ϵ	c	$k_s/[\eta]$
Compact sphere	0	0.667	0.333	0.333	~1.6
Rigid rod	1.8	0.15	0.85	1.0	<1 [a]
Random coil	0.5–0.8	0.4–0.5	0.5–0.6	0.5–0.6	~1.6

MHKS coefficients collated from [32].
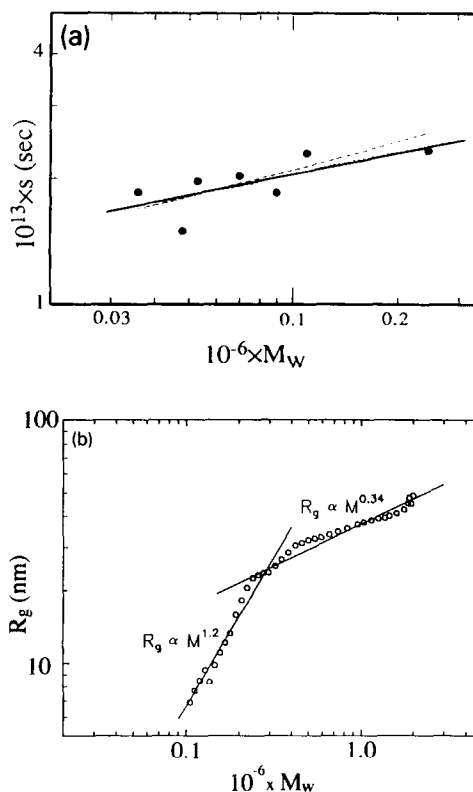[a] Depends on axial ratio.

Fig. 10. (a) Double logarithmic plot of sedimentation coefficient versus (weight average) molar mass (from sedimentation equilibrium) for a pectin polysaccharide (a polyanion). Solid line fitted corresponds to the MHKS Eq. (25), giving a $b = (0.17 \pm 0.07)$, consistent with a rigid rod model. Dashed line corresponds to the fit to a worm-like coil model with large persistence length: this is also only consistent with a rigid rod conformation. From [118]. (b) Double logarithmic plot of the radius of gyration versus (weight average) molar mass for amylose. Conformation "transition" from a rod to a more sphere-like structure occurs at an M_w of ~200000 g/mol. Molar mass determined by coupling a static light scattering detector to gel permeation chromatography according to [14]. From [113a].

pectin [118] showing a rigid rod conformation. An interesting application to the starch polysaccharide amylose of the c coefficient has been given by Rollings [113a] who demonstrated a conformation change from a rod to a more spherical structure above a molar mass of ca. 200000 g/mol (Fig. 10b). Other examples of applications to polysaccharides can be found in Ref. [33] and the source references cited therein.

7.2. Wales / van Holde ratio $k_s/[\eta]$

So named after the original paper of these authors [116]. Creeth and Knight [66] had collected a wide range of data for proteins and other macromolecules and shown that for globular particles, $k_s/[\eta] \sim 1.6$ and for more asymmetric particles < 1.6. This ratio (Table 8) was worked out for spheres, random coils, and subsequently (after several approximations and assumptions) in terms of ellipsoids of revolution by Rowe [61] who called this ratio the R-function. As noted above, R is a shape function which does not require an assumption concerning hydration. A value of 1.6 for spheres, which appears to agree with all the data [64–67,5], comes from the Einstein [37,38] value for $[\eta]$ of 2.5 v_s and a value for k_s of 4 v_s. The value '4' conflicted with an earlier value derived by Batchelor [117] of 6.55, (see Ref. [5] for a discussion on this) but the difference has been ascribed to one of definition – "is the sedimentation referring to one of movement through solution or solvent?", and how the effective viscosity of the solution is taken into account [61,67].

7.3. Haug triangle

In assessing the general conformation of macro-molecules using the MHKS or the Wales–van Holde relations a construction known as the Haug triangle has proved useful (Fig. 11). In this representation the three extremes of general conformation, each having specific values for the MHKS coefficients or $k_s/[\eta]$, are placed at the corners of this hypothetical triangle [32]. The general conformation of a given macro-molecule can then be represented by a locus along one of the sides between these three extremes. For example, a globular protein would be represented by a locus somewhere between the extremes of sphere
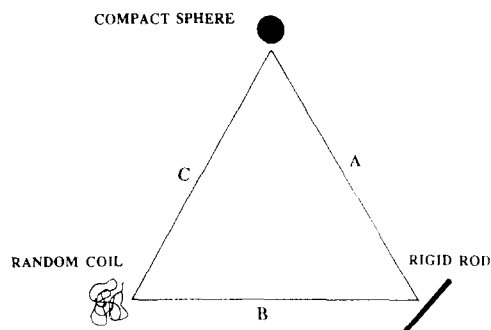

Fig. 11. Haug triangle representation of the gross conformation of macromolecules. From [32].

and rod (side A), a polysaccharide, DNA or a mucus glycoprotein between rod and coil (side B), a dena-tured protein between coil and sphere (side C). Table 9 gives some conclusions based on this representa-tion and $k_s/[\eta]$ and MHKS b coefficient data for three glycopolymers (an uncharged polysaccharide pullulan, a highly negatively charged polysaccharide pectin, and a mucin glycoprotein).

8. Modelling of flexible particles

There are two cases here: the first is that of segmentally flexible macromolecules, which is es-sentially an extension of the bead model theory to account for flexible joints or hinges (thereby facili-tating the modelling of myosin or immunoglobulins); the second applies more to linear macromolecular chains (like DNA and many polysaccharides) is worm-like coil models for continuous flexibility throughout the polymer chain.

Table 9
Gross conformation of three glycopolymers based on values for the MHKS b coefficient and $k_s/[\eta]$

	MHKS b	$k_s/[\eta]$	Conformation	Reference
Mucus glycoprotein	~ 0.4	~ 1.5	Random coil	[114]
Pullulans	0.45	~ 1.4	Random coil	[119]
Pectins	0.17	~ 0.2	Rigid rod	[118]

More examples can be found in [120].

8.1. Segmental flexibility models

A fuller description of this case can be found in Garcia de la Torre [30]. Segmental flexibility between domains or subunits of a molecule [121] has been considered in terms of completely flexible joints [122–127] or in terms of partial flexibility [128].

We have considered above how general ellipsoid modelling can give a good idea of the overall conformation without any prior assumption of conformation type (rod, disc etc.), and myosin was used for one of the examples. Iniesta et al. [129] have taken the myosin story a stage further: myosin has been well studied in terms of its hydrodynamic flexibility between the S2 head and the LMM region. The bending energy is given by [129]

$$(V/k_BT) = Q\alpha^2 \qquad (28)$$

where V is the bending potential (erg), α is the angle between the S2 and the LMM and Q is a dimensionless flexibility parameter. Good agreement was obtained from four different types of measurement (radius of gyration, electric birefringence decay constant, intrinsic viscosity and the longest relaxation time in electric birefringence ($\equiv \theta$)) for α and Q, giving mean values of $(58 \pm 4)°$ and $(0.56 \pm 0.13)°$ respectively, consistent with a moderate flexibility of the myosin rod (see, e.g. [30]).

8.2. Quasi-continuous flexibility: chain models and worm-like coil models

A fuller description of this can be found in Freire and Garcia de la Torre [34]. The simplest type of continuous flexibility is the unperturbed Gaussian chain and for long linear chains made up of N segments, and in this R_g varies as $N^{0.5}$, and if R_g is taken proportional to the Stokes or "hydrodynamic" radius, R_h, then the frictional coefficient f will also vary as $N^{0.5}$. If intramolecular excluded volume effects are taken into account between different parts of the chain, recent application of renormalization group theory gives

$$R_g \sim N^\nu \qquad (29)$$

where ν, is a critical exponent (not to be confused with the viscosity increment), and taking R_g proportional to R_h again, then

$$f \sim N^\nu \qquad (30)$$

This relation is supported by a substantial amount of experimental evidence (both $D_{20,w}$ and $s_{20,w}$ vary as $N^{-0.5}$). The Gaussian model involves, however, a number of crude oversimplifications, one of which is based on a value for ρ ($= R_g/R_h$) of 0.775, true only for rigid spheres. In fact for flexible polymers a value of $\rho \approx 1.3$ is found. Unfortunately there is no rigorous dynamic theory due to the fluctuating interactions between the chain elements. So-called "pre-averaging" approaches have led to moderate success [130,131] and are consistent with Eq. (30).

In cases where the polymer chain is non-linear through branching (comb structures, stars etc.), besides the ρ-parameter [11] the following ratios are useful [31,34]:

$$g = \frac{(R_g)^2}{(R_g^1)^2} \qquad (31)$$

$$h = \frac{f}{f^1} \qquad (32)$$

$$g' = \frac{[\eta]}{[\eta]^1} \qquad (33)$$

where "1" means the corresponding coefficient for the equivalent linear chain. This type of approach has found application in for example the study of branching in amylopectin ([113a] and references cited therein). Similar relations exist for cyclic or ring structures, where the respective ratios are q_s, q_f and q_η. In some ways these (g, h, g', q_s, q_f and q_η) are equivalent to the frictional ratio f/f_0 used in ellipsoid and rigid bead modelling, where the subscript "0" refers to a spherical particle of the same anhydrous volume as the particle and several relations between these ratios have been given (see, e.g. [132–135]).

8.3. Semi-flexible models: worm-like coils

This would apply to for example collagen, DNA and many polysaccharides: generally the more charged a polysaccharide is, the more rod-like its conformation. Thus highly charged polyanions like pectins and alginates, and polycations like chitosan have behaviour approaching that of stiff rods, whereas those of low or no charge behave more like random coils (such as pullulan or guar).

Such flexibility has been described in terms of so-called wormlike chain [136,34] and in terms of a variety of parameters, such as the ratio L/a, the ratio of the contour length of the chain to its persistence length. In the limits $L/a \to 0$ and $L/a \to \infty$ the conformation is rod-like and random coil respectively. Other criteria of flexibility used include for example the characteristic ratio, C_∞, the mass per unit length M_L and the "Kuhn statistical length" (with a variety of notations, such as "l_k", "σ^{-1}" or "λ^{-1}").

To assist in this type of modelling, again the dependence of R_g or hydrodynamic parameters on the molecular weight can be used to predict or model the L/a or equivalent parameters, and there have been many applications of these for modelling the stiffness/flexibility of:

- polysaccharides[11] such as carboxymethylcellulose [137], amylose and carboxymethylamylose [138], xanthan [139–141], hyaluronic acid [142–144], schizophyllan [145] alginate [143,146] and pectin [118,147];
- myosin filaments [148–153];
- DNA ([137], [154–157] and source references therein)
- filamentous viruses such as filamentous fd [158–160], the related M13 virus [161], and filamentous fd point mutants [162].

To quote some specific examples the theory of Yamakawa and Fuji [136] was recently used [118] to model the $[\eta]$ versus M data and the $s^0_{20,w}$ versus M data (dashed line of Fig. 10a) for citrus pectin, and the respective fits were consistent only with a rigid rod – again consistent with the MHKS and $k_s/[\eta]$ representations referred to above. Somewhat more flexibility was found by Porschke [157] for DNA, with models consistent with non-symmetric charge distributions. Bloomfield and co-workers ([154] and Refs. therein) have used dynamic light scattering translational diffusion coefficient measurements combined with imaging by electron microscopy to study the condensation of DNA under the influence of trivalent cations (hexamine cobalt(III)) and their effect on the conformation of the condensates (toroids or rods). Schurr and coworkers ([155] and Refs. therein) have also used dynamic light scattering diffusion measurements, together with sedimentation velocity and circular dichroism to show that inclu-

sion of a 16 base-pair fragment has a pronounced effect on the conformation of flanking residues stretching over several hundred base-pairs, dependent on the ionic strength. As our final example, Molina Garcia et al. [162] showed the frictional properties of the wild type filamentous virus fd could be approximated by those of a rigid rod used the relation of Tirado and Garcia de la Torre [110]

$$D^0_{20,w} = (k_B T/3\pi\eta_0 L)(\ln(L/d) + \gamma) \qquad (34)$$

(where d is the thickness of the fd virus chain and γ is a small end correction term) to compare a difference in contour length and possibility flexibility of two point-mutants of fd. The virtue of combining translational diffusion (or sedimentation coefficient) with rotational diffusion and other measurements was clearly indicated.

9. Glossary of symbols

a,b, semi-axes of an ellipsoid of revolution ($a \geq b$); a,b,c, semi axes of a general triaxial ellipsoid ($a \geq b \geq c$); w, hydration (g/g: i.e. number of grams of solvent bound per gram of macromolecule); V, particle volume (including, where appropriate, associated solvent or "hydration") (ml); $\bar{v}$, partial specific volume (ml/g); v_s, swollen specific volume (ml/g), α_i ($i = 1–10$), elliptic integrals; P, Perrin function ("frictional ratio due to shape"); ν, viscosity increment; u_{red}, $\theta^{red}_\pm$, τ_h/τ_0, τ_i/τ_0, other shape parameters requiring knowledge of hydration information (i.e. w or v_s) for their experimental determination; β, Ψ, ψ, R, Λ and Π, G, $\delta_\pm$ shape parameters not requiring knowledge of w or v_s.

a,b,c and ϵ, exponents in the MHKS viscosity, sedimentation, radius of gyration and translational diffusion equations respectively.

a, persistence length (cm); L, contour length (cm); Q, flexibility parameter; V, bending potential (erg); g, h, g': branching parameters; q_s, q_f, q_h, ring or cyclic parameters; d, thickness of a rod model (cm).

c, concentration (g/ml); $D_{20,w}$, apparent translational diffusion coefficient (cm^2/s) at a finite concentration, c, and corrected to standard solvent conditions (i.e. water as solvent at a temperature of $20.0°$ C); $D^0_{20,w}$, "infinite" dilution translational diffusion coefficient (cm^2/s); $s_{20,w}$, apparent sedimen-

tation coefficient (s or S) at a finite concentration, c, and corrected to standard solvent conditions (i.e. water as solvent at a temperature of 20.0° C); $s_{20,w}^0$, "infinite" dilution sedimentation coefficient (s or S); M, molar mass (g/mol); N_A, Avogadro's number (mol^{-1}); (f/f_0), frictional ratio. Following the most popular convention [3], f_0 refers to the frictional coefficient of a spherical particle of the same mass and *anhydrous* volume as the macromolecule whose frictional coefficient is f. This differs from the usage of for example Scheraga and Mandelkern [55] and from some of our earlier papers (see e.g. Refs. [27,28]) where f_0 refers to a sphere of the same *hydrated* volume; U, molar covolume (ml/mol); B (or A_2), thermodynamic ("osmotic pressure") second virial coefficient (ml · mol · g^{-2}); Z, charge on a macromolecule; I, ionic strength (mol/l or mol/ml); k_B, Boltzmann constant (erg · K^{-1}); T, absolute temperature (K); τ_h, harmonic mean rotational relaxation time (s); ρ_0, solution or solvent density (g/ml); η_0, solvent viscosity (poise); $[\eta]$, intrinsic viscosity (ml/g); θ_i, electric birefringence decay constants (s^{-1}) (two for a monodisperse solution of homogeneous triaxial ellipsoids); R_g, radius of gyration (cm); R_h Stokes or "hydrodynamic" radius (cm); k_s, concentration dependence sedimentation regression parameter (ml/g).

References

[1] H.K. Schachman, Nature (1989) 259.

[2] H.K. Schachman, C.D. Pauza, M. Navre, M.J. Karela, L. Wu and Y.R. Yang, Proc. Natl. Acad. Sci. USA, 81 (1984) 115.

[3] C. Tanford, Physical Chemistry of Macromolecules, J. Wiley, New York, 1961.

[4] K. Jumel, PhD Dissertation, University of Nottingham, UK, 1994.

[5] S.E. Harding and P. Johnson, Biochem. J., 231 (1985) 543; Biochem. J., 231 (1985) 549.

[6] R.L. Whorlow, Rheological Techniques, 2nd ed., Ellis Horwood, Chichester, UK, 1993.

[7] R. Giebler, in S.E. Harding, A.J. Rowe and J.C. Horton (Editors), Analytical Ultracentrifugation in Biochemistry and Polymer Science, Royal Society of Chemistry, Cambridge, UK, 1992, p. 16.

[8] W. Brown, Dynamic Light Scattering. The Method and Some Applications, Oxford University Press, 1993.

[9] R.M. Johnsen and W. Brown, in Laser Light Scattering in Biochemistry, Royal Society of Chemistry, Special Publication no. 99, Cambridge, UK, p. 77.

[10] P. Stepanek, in W. Brown (Editor), Dynamic Light Scattering. The Method and Some Applications, Clarendon Press, Oxford, 1993, p. 177.

[11] W. Burchard, in Laser Light Scattering in Biochemistry, Royal Society of Chemistry, Special Publication no. 99, Cambridge, UK, 1992, p. 3; W. Burchard, Chimia, 39 (1985) 10.

[12] B.H. Zimm, J. Chem. Phys. 16 (1948) 1099.

[13] S.E. Harding, D.B. Sattelle and V.A. Bloomfield, Laser Light Scattering in Biochemistry, Royal Society of Chemistry, Special Publication no. 99, Cambridge, UK, 1992.

[14] P.J. Wyatt, in Laser Light Scattering in Biochemistry, Royal Society of Chemistry, Special Publication no. 99, Cambridge, UK, 1992, p. 35.

[15] C.L. Riddiford and B. Jennings, Biopolymers, 5 (1967) 757.

[16] E. Fredericq and C. Houssier, Electric Dichroism and Electric Birefringence, Clarendon Press, Oxford, UK, 1973.

[17] C.R. Cantor and T. Tao, Proc. Nucl. Acid Res., 2 (1971) 31.

[18] D. Ridgeway, J. Am. Chem. Soc., 90 (1968) 18.

[19] E.W. Small and I. Isenberg, Biopolymers, 16 (1977) 1907.

[20] I. Isenberg and E.W. Small, J. Chem. Phys., 77 (1982) 2799.

[21] D.Porschke and A. Obx, Rev. Sci., Instrum., 62 (1991) 818.

[22] P. Johnson and E. Mihalyi, Biochim. Biophys. Acta, 102 (1965) 476.

[23] A. Dell, Adv. Carbohydr. Chem. Biochem., 45 (1987) 19.

[24] S.E. Harding, Methods Mol. Biol., 22 (1994) 75.

[25] S.J. Perkins, Eur. J. Biochem., 157 (1986) 169.

[26] O. Kratky, H. Leopold and H. Stabinger, Methods Enzymol., 27 (1973) 98.

[27] S.E. Harding and A.J. Rowe, Int. J. Biol. Macromol., 4 (1982) 160.

[28] S.E. Harding, PhD Thesis, University of Leicester, UK, 1980.

[29] S.E. Harding, in Dynamic Properties of Biomolecular Assemblies, Royal Society of Chemistry, Special Publication no. 74, Cambridge, UK, 1989, p. 32.

[30] J. Garcia de la Torre, in Dynamic Properties of Biomolecular Assemblies, Royal Society of Chemistry, Special Publication no. 74, Cambridge, UK, p. 3.

[31] J. Garcia de la Torre, in S.E. Harding, A.J. Rowe and J.C. Horton (Editors), Analytical Ultracentrifugation in Biochemistry and Polymer Science, Royal Society of Chemistry, Cambridge, UK, 1992, p. 333.

[32] O. Smidsrød and I.L. Andresen, Biopolymerkjemi, Tapir, Trondheim, Norway, 1979.

[33] S.E. Harding, K.M. Vårum, B.T. Stokke and O. Smidsrød, Adv. Carbohydr. Analys., 1 (1991) 63.

[34] J.J. Freire and J. Garcia de la Torre, in S.E. Harding, A.J. Rowe and J.C. Horton (Editors), Analytical Ultracentrifugation in Biochemistry and Polymer Science, Royal Society of Chemistry, Cambridge, UK, 1992, p. 346.

[35] G. Stokes, Trans. Cambridge Phil. Soc., 8 (1847) 287 and 9 (1851) 8.

[36] A.Einstein, Ann. Physik., 19 (1906) 289 and *corrigenda* 34 (1911) 591.

[37] A. Einstein, in R. Furth (Editor), Investigations of the Theory of Brownian Movement, Dover Publications, New York, NY, 1956.

[38] F. Perrin, J. Phys. Radium, 7 (1936) 1.

[39] T. Svedberg and H. Rinde, J. Am. Chem. Soc., 45 (1923) 943.

[40] T. Svedberg and O. Pedersen, The Ultracentrifuge, Oxford University Press, Oxford, 1940, and references cited therein.

[41] T. Laue, B.D. Shah, T.M. Ridgeway and S.L. Pelletier, in S.E. Harding, A.J. Rowe and J.C. Horton (Editors), Analytical Ultracentrifugation in Biochemistry and Polymer Science, Royal Society of Chemistry, Cambridge, UK, 1992, p. 90.

[42] F. Perrin, J. Phys. Radium, 5 (1934) 497.

[43] R. Simha, J. Phys. Chem., 44 (1940) 25.

[44] G.B. Jeffery, Proc. R. Soc. London, Ser. A, 102 (1922) 161.

[45] N. Saito, J. Phys. Soc. Japan, 6 (1951) 297.

[46] S.E. Harding, M. Dampier and A.J. Rowe, Biophys. Chem., 15 (1982) 205.

[47] NAG, The NAG FORTRAN Workstation Library Handbook – Release 1, The Numerical Algorithms Group Limited, Jordan Hill Road, Oxford, UK, 1986.

[48] C. Tanford, Physical Chemistry of Macromolecules, J. Wiley and Sons, New York, NY, 1961, Chap. 6.

[49] A.G. Ogston and D.J. Winzor, J. Phys. Chem., 79 (1975) 2496.

[50] L. W. Nichol, P.D. Jeffrey and D.J. Winzor, J. Phys. Chem., 80 (1976) 648.

[51] H. Benoit, Ann. Phys., 6 (1951) 561.

[52] G. Weber, Adv. Prot. Chem., 8 (1953) 415.

[53] S.E. Harding, A.J. Rowe and J.M. Creeth, Biochem. J., 209 (1983) 893.

[54] P.G. Squire and M. Himmel, Arch. Biochem. Biophys., 196 (1979) 165.

[55] H.A. Scheraga and L. Mandelkern, J. Am. Chem. Soc., 79 (1953) 179.

[56] J.L. Oncley, Ann. N.Y. Acad. Sci., 41 (1941) 121.

[57] S.E. Harding, Biochem. J., 189 (1980) 359.

[58] P.G. Squire, Biochim. Biophys. Acta, 221 (1970) 425.

[59] P.G. Squire, Electro-Opt. Ser., 2 (1978) 569.

[60] P.D. Jeffrey, L.W. Nichol, D.R. Turner and D.J. Winzor, J. Phys. Chem., 81 (1977) 776.

[61] A.J. Rowe, Biopolymers, 16 (1977) 2595. See also A.J. Rowe, in S.E. Harding, A.J. Rowe and J.C. Horton (Editors), Analytical Ultracentrifugation in Biochemistry and Polymer Science, Royal Society of Chemistry, Cambridge UK, 1992, p. 394.

[62] S.E. Harding, Int. J. Biol. Macromol., 3 (1981) 340.

[63] M. Rholam and P. Nicolas, Biochemistry, 20 (1981) 5837.

[64] P.Y. Cheng and H.K. Schachman, J. Polym. Sci., 16 (1955) 1930.

[65] H.K. Schachman, Ultracentrifugation in Biochemistry, Academic Press, New York, NY, 1959, Chap. 4.

[66] J.M. Creeth and C.G. Knight, Biochim. Biophys. Acta, 102 (1965) 549.

[67] P.N. Lavrenko, K.J. Linow and E. Görnitz, in S.E. Harding, A.J. Rowe and J.C. Horton (Editors), Analytical Ultracentrifugation in Biochemistry and Polymer Science, Royal Society of Chemistry, Cambridge, UK, 1992, p. 517.

[68] S.E. Harding and H. Cölfen Anal. Biochem., (1995) in press.

[69] E.W. Small and I. Isenberg, Biopolymers, 16 (1977) 1907.

[70] J.M. Rallison, J. Fluid Mech., 84 (1978) 237.

[71] S.E. Harding, M. Dampier and A.J. Rowe, IRCS Med. Sci., 7 (1979) 33.

[72] S.E. Harding, M. Dampier and A.J. Rowe, J. Colloid Interface Sci., 79 (1981) 7.

[73] J.M. Rallison and S.E. Harding, J. Colloid Interface Sci., 103 (1985) 284.

[74] S.H. Haber and H. Brenner, J. Colloid Interface Sci., 97 (1984) 496.

[75] S.E. Harding and A.J. Rowe, Int. J. Biol. Macromol., 4 (1982) 161.

[76] W.A. Wegener, Biopolymers, 23 (1984) 2243.

[77] W.A. Wegener, R.M. Dowben and V.J. Koester, J. Chem. Phys., 70 (1979) 622.

[78] S.E. Harding, Comput. Biol. Med., 12 (1982) 75.

[79] H.A. Scheraga, Protein Structure, Academic Press, New York, NY, 1961.

[80] S.E. Harding, Biophys. J., 51 (1987) 673.

[81] D. Ridgeway, J. Am. Chem. Soc., 88 (1966) 1104.

[82] P. R. Wills, L. Nichol and R.J. Siezen, R.J., Biophys. Chem., 11 (1980) 71.

[83] S.E. Harding and A.J. Rowe, Biopolymers, 22 (1983) 1813 and 23 (1984) 843.

[84] M.K. Han, J.R. Knutson and L. Brand, in Dynamic Properties of Biomolecular Assemblies, Royal Society of Chemistry, Special Publication no. 74, Cambridge, UK, 1989, p. 115.

[85] A.K. Livesey and J. Brochon, in Dynamic Properties of Biomolecular Assemblies, Royal Society of Chemistry, Special Publication no. 74, Cambridge, UK, 1989, p. 135.

[86] H. Mark, Der feste Körper, Hirzel, Leipzig, 1938, p. 103; R. Houwink J. Prakt. Chem., 157 (1941) 15; W. Kuhn and H. Kuhn, Helv. Chim. Acta, 26 (1943) 1394; I. Sakurada, Kasen Koenshu, 5 (1940) 33 and 6 (1941) 177.

[87] J.G. Grössmann, Z.H.L. Abraham, E.T. Adman, M. Neu, R.R. Eady, B.E. Smith and S.S. Hasnain, Biochemistry, 32 (1993) 7360.

[88] S.E. Harding, Adv. Carbohydr. Chem. Biochem., 47 (1989) 345.

[89] S.E. Harding, Biochem. Soc. Trans., 14 (1986) 857.

[90] S.E. Harding, Comput. Biol. Med., 13 (1983) 89.

[91] V.A. Bloomfield, W.D. Dalton and K.E. van Holde, Biopolymers, 5 (1967) 135.

[92] J.G. Kirkwood, J. Polym. Sci., 12 (1954) 1.

[93] J. Garcia de la Torre and V.A. Bloomfield, Biopolymers, 16 (1977) 1779.

[94] J. Antosiewicz and D.Porschke, Biophys. Chem., 33 (1989) 19.

[95] D. Porschke and J. Antosiewicz, in Dynamic Properties of Biomolecular Assemblies, Royal Society of Chemistry, Special Publication no. 74, Cambridge, UK, 1989, p. 103.

[96] S.J. Perkins, in Dynamic Properties of Biomolecular As-

semblies, Royal Society of Chemistry, Special Publication no. 74, Cambridge, UK, 1989, p. 226.

[97] P.J. Morgan, O.D. Byron and S.E. Harding, Discovery, 1 (1992) 2.

[98] P. Plietz, G. Damaschun, J.J. Müller and K.-D. Schwenke, Eur. J. Biochem., 130 (1983) 315.

[99] L. Gregory, K.G. Davis, B. Sheth, J. Boyd, R. Jefferis, C. Nave and D.R. Burton, Mol. Immunol.. 24 (1987) 821.

[100] O.D. Byron, PhD Dissertation, University of Nottingham, UK, 1992.

[101] O.D. Byron and S.E. Harding, ms.in preparation.

[102] J. Garcia de la Torre and V.A. Bloomfield, Biopolymers, 16 (1977) 1747.

[103] J. Garcia de la Torre and V.A. Bloomfield, Biopolymers, 16 (1977) 1765.

[104] J. Garcia de l Torre, M.C. Lopez Martinez and J.J. Garcia Molina, Macromolecules, 20 (1987) 661; J. Garcia de la Torre, in S. Krause (Editor), Molecular Electro-Optics, Plenum, New York, 1981, p. 75.

[105] K. Tsuda, Rheol. Acta, 9 (1970) 509; Polym. J., 1 (1970) 616.

[106] J.J. Freire and J. Garcia de la Torre, Macromolecules, 16 (1983) 331.

[107] J. Garcia de la Torre and V.A. Bloomfield, Biopolymers, 17 (1978) 1605.

[108] J. Garcia de la Torre and V.A. Bloomfield, Q. Rev. Biophys., 14 (1981) 81.

[109] E. Swanson, D.C. Teller and C. de Haen, J. Chem. Phys., 68 (1978) 5097.

[110] M.M. Tirado and J. Garcia de la Torre, J. Chem. Phys., 71 (1979) 2581 and 73 (1980) 1986.

[111] J. Garcia de la Torre, M.C. Lopez Martinez and M.M. Tirado, Biopolymers, 23 (1984) 611; J. Chem. Phys., 81 (1984) 2047.

[112] R.P. Roger and R.G. Husey, Phys. Fluids, 25 (1982) 915.

[113] S.A. Allison, R.A. Easterly and D.C. Teller, Biopolymers, 19 (1980) 1475; 113a J.E. Rollings, in Laser Light Scattering in Biochemistry, Royal Society of Chemistry, Special Publication no. 99, Cambridge UK, 1989, p. 275.

[114] J.K. Sheehan and I. Carlstedt, Biochem. J., 217 (1984) 93.

[115] J.K. Sheehan and I. Carlstedt, in Dynamic Properties of Biomolecular Assemblies, Royal Society of Chemistry, Special Publication no. 74, Cambridge, UK, 1989, p. 256; [115a] A.M. Jamieson, J. Blackwell, D. Zangrando and A. Demers, in Laser Light Scattering in Biochemistry, Royal Society of Chemistry, Special Publication no. 99, Cambridge, UK, 1992, p. 260.

[116] M. Wales and K.E. van Holde, J. Polym. Sci., 14 (1954) 81.

[117] G.K. Batchelor, J. Fluid Mech., 52 (1972) 245.

[118] S.E. Harding, G. Berth, A. Ball, J.R. Mitchell and J. Garcia de la Torre, Carbohydr. Polym., 16 (1991) 1.

[119] K. Kawahara, K. Ohta, H. Miyamoto and S. Nakamura, Carbohydr. Polym., 4 (1984) 335.

[120] S.E. Harding, in S.E. Harding, A.J. Rowe and J.C. Horton (Editors), Analytical Ultracentrifugation in Biochemistry and Polymer Science, Royal Society of Chemistry, Cambridge, UK, 1992, p. 495.

[121] J. Yguerabide, H.F. Epstein and L. Stryer, J. Mol. Biol., 51 (1970) 573.

[122] W.A. Wegener, R.M. Dowben and V.J. Koester, J. Chem. Phys., 73 (1980) 4086.

[123] W.A. Wegener, Biopolymers, 21 (1982) 1409; J. Chem. Phys., 76 (1982) 6425.

[124] S.C. Harvey, P. Mellado and J. Garcia de la Torre, J. Chem. Phys., 78 (1983) 2081.

[125] J. Garcia de la Torre, P. Mellado and V. Rodes, Biopolymers, 24 (1985) 2145.

[126] W.A. Wegener, Macromolecules, 18 (1985) 2522.

[127] A. Iniesta and J. Garcia de la Torre, Eur. Biophys. J., 14 (1987) 493.

[128] D.B. Roitman and B.H. Zimm, J. Chem. Phys., 81 (1984) 6333 and 81 (1984) 6348.

[129] A. Iniesta, F.G. Diaz and J. Garcia de la Torre, Biophys. J. 54 (1989) 269.

[130] B.H. Zimm, Macromolecules, 13 (1980) 592.

[131] M. Fixman, J. Chem. Phys., 84 (1986) 4080.

[132] H. Yamakawa, Modern Theory of Polymer Solutions, Harper and Row, New York, NY, 1971.

[133] R. Prats, J. Pla and J.J. Freire, Macromolecules, 16 (1983) 1701.

[134] J. M. Garcia Bernal, M.M. Tirado, J.J. Freire and J. Garcia de la Torre, Macromolecules, 23 (1990) 3357.

[135] J. M. Garcia Bernal, M.M. Tirado, J.J. Freire and J. Garcia de la Torre, Macromolecules, 24 (1991) 593.

[136] J.E. Hearst and W.H. Stockmayer, J. Chem. Phys., 37 (1962) 1425; H. Yamakawa and M. Fujii, Macromolecules 6 (1973) 407; H. Yamakawa and M. Fujii, Macromolecules 7 (1974) 128; C. R. Cantor and P.R. Schimmel, Biophysical Chemistry, Freeman, New York, NY, 1979.

[137] M. Tricot, Macromolecules, 17 (1984) 1698.

[138] H. Yamakawa, Ann. Rev. Phys. Chem. 35 (1984) 23.

[139] T. Sato, T. Norisuye and H. Fujita, Macromolecules 17 (1984) 2696.

[140] L. Zhang, W. Liu, T. Norisuye and H. Fujita, Biopolymers 26 (1987) 333.

[141] G. Holzwarth, Carbohydr. Res. 66 (1978) 173.

[142] R.L. Cleland and J.L. Wang, Biopolymers, 9 (1970) 799.

[143] A. Gamini, S. Paoletti and F. Zanetti, in Laser Light Scattering in Biochemistry, Royal Society of Chemistry, Special Publication no. 99, Cambridge, UK, 1992, p. 294.

[144] R.L. Cleland, Biopolymers 23 (1984) 647.

[145] Y. Kashiwagi, T. Norisuye and H. Fujita, Macromolecules 14 (1981) 1220.

[146] O. Smidsrød, Carbohydr. Res. 13 (1970) 359.

[147] S.E. Harding, G. Berth, A. Ball and J.R. Mitchell, Gums Stabilisers Food Ind., 5 (1990) 267.

[148] N. Mochizuki-Oda and S. Fujime, Biopolymers, 27 (1988) 1389.

[149] N. Suzuki and A. Wada, Biochim. Biophys. Acta, 670 (1981) 408.

[150] K. Kubota, B. Chu, S.-F. Fan, M.M. Dewey, P. Brink and D.E. Colflesh, J. Mol. Biol., 166 (1983) 329.

[151] S. Fujime and K. Kubota, Macromolecules, 17 (1984) 441.

[152] S.-F. Fan, M.M. Dewey, D. Colflesh, B. Gaylinn, R. Greguski and B. Chu, Biophys. J., 47 (1985) 809.

[153] S. Fujime and N. Mochizuki-Oda, in Laser Light Scattering in Biochemistry, Royal Society of Chemistry, Special Publication no. 99, Cambridge, UK, 1992, p. 245.

[154] V. A. Bloomfield, S. He, A.-Z. Li and P.G. Arscott, in Laser Light Scattering in Biochemistry, Royal Society of Chemistry, Special Publication no. 99, Cambridge, UK, 1992, p. 320.

[155] J.M. Schurr, U.-S. Kim, L. Song, B.S. Fujimoto, C.E. Furlong and J.A. Sundstrom, in Laser Light Scattering in Biochemistry, Royal Society of Chemistry, Special Publication no. 99, Cambridge, UK, 1992, p. 334.

[156] R. Pecora, in Laser Light Scattering in Biochemistry, Royal Society of Chemistry, Special Publication no. 99, Cambridge, UK, 1992, p. 354.

[157] D. Porschke, Biophys. Chem., 49 (1994) 127.

[158] S. Fujime and T. Maeda, Macromolecules, 18 (1985) 191.

[159] J. Newman, H.L. Swinney and L.A. Day, J. Mol. Biol., 116 (1977) 593.

[160] L. Day and R.L. Wiseman, in D.T. Denhardt, D. Dressler and D.S. Ray (Editors), The Single Stranded DNA Phages, Cold Spring Harbor Laboratory, New York, 1978, p. 605.

[161] L. Song, U.-S. Kim, J. Wilcoxon and J.M. Schurr, Biopolymers, 31 (1991) 547.

[162] A.D. Molina-Garcia, S.E. Harding, F.G. Diaz, J. Garcia de la Torre, D. Rowitch and R.N. Perham, Biophys. J., 63 (1992) 1293.